

Background Document

FEMA P-58/BD-3.7.14

PACT Beta Test Example: Building A Steel Special Moment Frame Building

Prepared by

Farzin Zareian

Dept. of Civil & Environmental Engineering
University of California, Irvine
Irvine, California 92697

Submitted to

APPLIED TECHNOLOGY COUNCIL
201 Redwood Shores Parkway, Suite 240
Redwood City, California 94065
www.ATCouncil.org

Prepared for

FEDERAL EMERGENCY MANAGEMENT AGENCY
U.S. Department of Homeland Security
500 C Street, SW
Washington, D.C. 20472

March 23, 2012



FEMA



Background Documentation

FEMA P-58 Background Documents are a series of reports documenting the technical background and source information for key aspects of the FEMA P-58 methodology and its implementation. These reports were developed over the course of the 10-year ATC-58/ATC-58-1 Projects funded under FEMA Contracts EMW-2001-RP-0056 and HSFEHQ-06-D-1105.

Background Documents were developed by consultants, serving at various levels within the project hierarchy, reporting the results of: (1) decisions on technical development protocols; (2) focused studies on the development of key aspects of the methodology; (3) documentation of recommended procedures; and (4) collection of available data for the development of structural and nonstructural fragilities. They were initially intended to serve as a record of the technical state-of-knowledge at the time they were produced, and as resources for the development of the eventual project reports. As such, they represent a snapshot in time, and may, or may not, match the technical content, recommended procedures, or data incorporated into the final methodology and its implementation.

This Background Document is intended for the purpose of providing supplemental knowledge to users of the FEMA P-58 methodology. Information contained herein has not been independently verified for accuracy as a stand-alone document, and may have been superseded in its final implementation within the methodology. Users of information in this document assume all liability arising from such use.

Notice

Any opinions, findings, conclusions, or recommendations expressed in this publication do not necessarily reflect the views of the Applied Technology Council (ATC), the Department of Homeland Security (DHS), or the Federal Emergency Management Agency (FEMA). Additionally, neither ATC, DHS, FEMA, nor any of their employees, makes any warranty, expressed or implied, nor assumes any legal liability or responsibility for the accuracy, completeness, or usefulness of any information, product, or process included in this publication. Users of information from this publication assume all liability arising from such use.

Cover illustration – Primary resource documents for the FEMA P-58 *Seismic Performance Assessment of Buildings, Methodology and Implementation* series of products: FEMA P-58-1, *Volume 1 – Methodology*, and FEMA P-58-2, *Volume 2 – Implementation Guide*.

PACT Beta Test Example: Building A Steel Special Moment Frame Building

Prepared by
Farzin Zareian
University of California, Irvine

March 23, 2012

1.1 Steel Special Moment Frame Example

1.1.1 Introduction and Overview

This study addresses the application of the ATC-58 loss estimation methodology using the PACT software for estimation of losses of an 8-story research laboratory building denoted as Building A. The lateral load resisting system of Building A comprises Special Moment Resisting Frames and is located in Sacramento (California) with a Seismic Design Category D_{min} ($SDC = D_{min}$). The intention of this study is to investigate the sensitivity of the probabilistic representation of estimated losses (i.e., Repair Cost, and Repair Time) to variation in various parameters used in the loss estimation process.

1.1.2 Description of Building and Site

Building A is an 8-story building located in Sacramento, California. The lateral load resisting system of this building comprise 3-bay special moment resisting frames (SMRF) as shown in Figure 1-1. The centerline dimension between columns is 20', the height of the first story is 15', and heights of all other stories are 13'. This building is one of the many Steel SMRFs designed for a study for assessing the collapse safety of Steel SMRF using the FEMA P695 methodology (Zareian et. al., 2010). More information about the site and seismic hazard is provided in the PACT Beta Test Overview Report, BD-3.7.13.

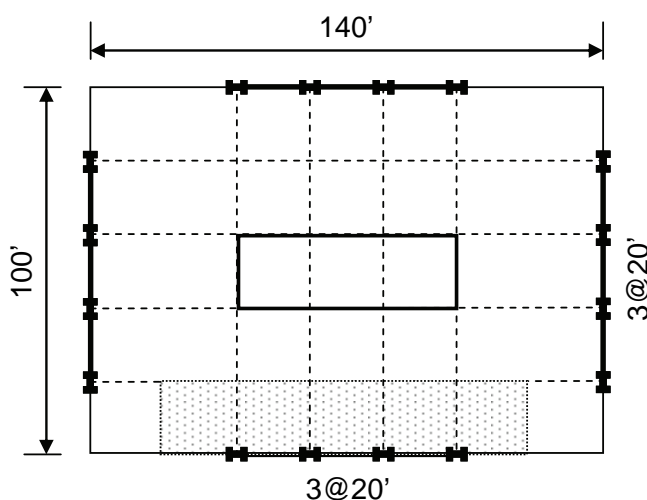


Figure 1-1 Plan view of Building A

Building A is designed for a dead load of 90 psf, cladding load on the perimeter of 25 psf, and unreduced live load of 50 psf on all floors (20 psf on

roof). All beam-column connections are RBS designed in accordance with AISC 358-05, using $a = 0.625b_f$, $b = 0.75d_b$, and $c = 0.250b_f$.

Building A is designed in accordance with building codes: ASCE 7-05 and AISC 341-05. The only exception to ASCE 7-05 is the use of $C_d = R = 8$ and wind loads are not considered. Column splices are provided every two stories and end columns may be of different size than interior columns. All three beams at a floor level are of the same size.

Due to low values of ground motion intensity at the design level, and using the response spectrum analysis in the design process, Building A is a flexible structure with first mode period of 3.55 seconds. The design was governed by ASCE 7-05 P-Delta stability requirements. The building has an overstrength factor of 2.7.

1.1.3 Documentation of PACT Input

Information required for performing loss estimation using PACT needs to be completely input into the program using the PACT Building Manager (activated in the PACT Control Panel under the title “Model the Building and Import Analysis Results” button). The Building Manager is an easy to use windows-based program and takes the required information in various tabs: Project Info, Building Info, Population, Fragilities, Performance Groups, Collapse Fragility, Structural Analysis Results, Residual Drift, and Hazard Curve. In the following the sequence of inputting information in these tabs are described.

1.1.3.1 Project Information tab

The first tab, Project Info, is where the user inputs general information about the project in hand. Among the information input here is the Engine Random Seed Value and Calculation Red Tags on/off switch. If a value of zero is selected for the seed value, then PACT generates new sets of random numbers each time it is asked to run the loss estimation process. A value other than zero for the seed value will force the program to use a specific set of random numbers. This specific set of random numbers only depend the seed value and the computer that is running the analysis. However, we did look into the effect of turning the Red Tag calculation switch to on and off. Our investigation shows that turning the activation switch to off (i.e., NOT calculating the Red Tag during the loss assessment process) can reduce the time required to do the loss estimation by the PACT engine.

Given the generic nature of this effort, the Region Cost Multiplier and Date Cost Multiplier were set equal to unity. However, application of PACT for assessing losses of a target structure should consider the surge in the regional

costs of labor, cost of construction materials, and associated delays in seismic events.

1.1.3.2 Building Information tab

The second tab, Building Info, is where information about the building’s total replacement cost and replacement time, cost of replacing the core and shell (structural elements), max workers per square feet, and information about each floor of the building is input. Figure 1-2 shows this tab for Building A. We estimated the total replacement cost of the building to be equal to \$39,200,000 (that is \$350 per square feet for the gross square footage of Building A: $8 \times 14,000 = 112,000 \text{ ft}^2$). We assumed 30% of the replacement cost is the cost of replacing the Core and Shell (e.g., \$11,760,000). For the Replacement Time and Maximum Workers per square feet we used 720.0 and 0.002, respectively, following the advice of the project advisory team.

Pact 2 Building Manager - 8-story Laboratory Building in Sacramento

File Edit Tools Help

Project Info Building Info Population Fragilities Performance Groups Collapse Fragility Structural Analysis Results Residual Drift Hazard Curve

Number of Stories: 8

Total Replacement Cost (\$): 39,200,000 Replacement Time (days): 720.00 Total Loss Threshold (As Ratio of Total Replacement Cost): 1

Core and Shell Replacement Cost (\$): 11,760,000 Max Workers per sq. ft.: 0.002

Most Typical Defaults

Floor Area (sq. ft.): 14,000.00 Floor Height (ft.): 13

Floor Num	Floor Name	Story Height (ft.)	Area (sq. ft.)	Height Factor	Hazmat Factor	Occupancy Factor
1	Floor 1	15.00	14,000.00	1	1	1
2	Floor 2	13.00	14,000.00	1	1	1
3	Floor 3	13.00	14,000.00	1	1	1
4	Floor 4	13.00	14,000.00	1	1	1
5	Floor 5	13.00	14,000.00	1	1	1
6	Floor 6	13.00	14,000.00	1	1	1
7	Floor 7	13.00	14,000.00	1	1	1
8	Floor 8	13.00	14,000.00	1	1	1
9	Floor 9		14,000.00	1	1	1

Figure 1-2 PACT input in “Building Information” tab for Building A

1.1.3.3 Building Information tab

In the third tab, Population, we assumed Building A is a “Research” type facility in all floors (The fraction of each floor that was modeled as “Research” was 1.0). The “Peak number of occupants per 1000sf” and “Population Dispersion” was considered to be 4.0 and 0.2, respectively, per PACT default values. Figure 1-3 shows a screen shot of this tab for Building A. The values are available from the library of occupancy types within PACT.

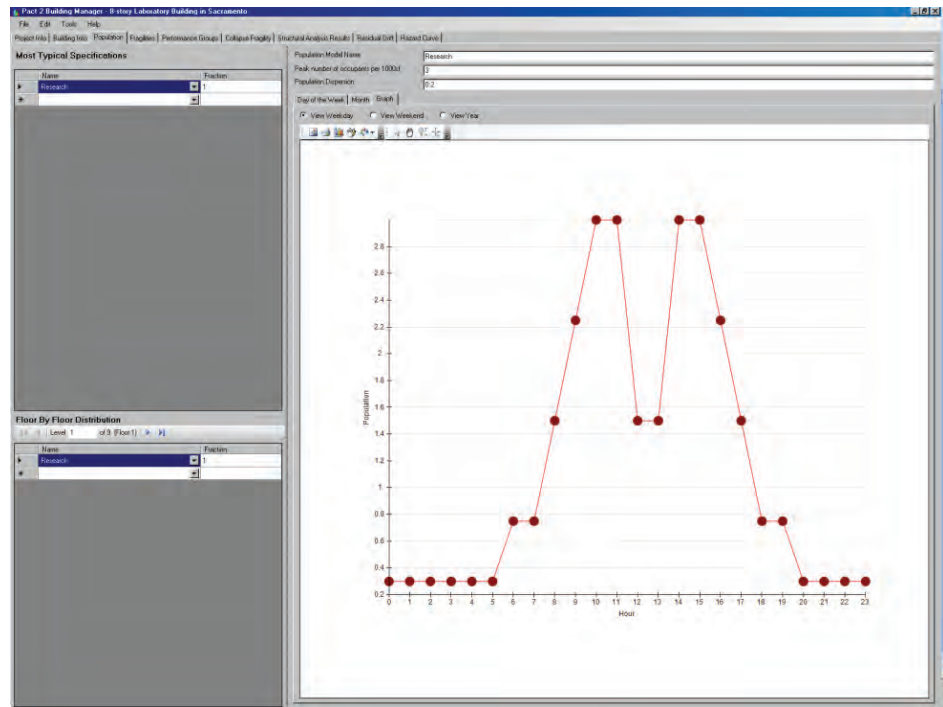


Figure 1-3 PACT input in “Population” tab for Building A

1.1.3.4 Fragilities and Performance Groups

The Fragilities tab in the PACT Building Manager is used to populate the performance groups in the Performance Groups tab. Only the type of performance group is selected here and the quantities are input later in the Performance Group tab. Performance groups are divided into directional and non-directional; we assumed the left-right direction is Dir 1, and the up-down direction is Dir 2. The user can also edit the .xml file associated with the project and populate the Performance Group tab with appropriate information (in fact the later was used for the purpose of this effort).

Table 1-1 and 1-2 show the calculations for the quantities we input in the Performance Group tab for Building A for contents, and structural components, respectively. The quantities for each performance group in Building A in Table 1-1 is obtained by multiplying the 50% Quantities of Normative Values in Appendix F of ATC-58 90% report by corresponding measurements for that building. Few rows in Table 1-1 are shaded showing the performance groups that were not used in the Building A model for one of the following reasons: a) PACT engine error if that particular performance group was used, b) fragility curve for that particular performance group was not available. The last column in Table 1-1 shows the performance group fragility number or the reason why that particular performance group was not used.

Table 1-1 Performance Group Calculations for Building A

Normative Quantity Type	Unit of Measurement	50% Quantity	Measurement for Bldg. A	Quantity for Bldg. A	PACT Perf. Group
Gross Wall Area	SF per 1 gsf	0.520	0.0	0.0	---
Windows or Glazing Area	100 SF per 1 gsf	1.5E-03	Based on perimeter cladding size	140 (Dir 1, FL. 1) 100 (Dir 2, FL. 1) 122 (Dir 2, other) 87 (Dir 2, other)	B2022.001a
Roof Area - Total	SF per 1 gsf	0.245	NOT USED (PACT error)	34.3	B3011.011
Interior Partition Length	100 LF per 1 gsf	8.5E-04	14000X0.58 (Dir 1) 14000X0.42 (Dir 2)	6.9 (Dir 1) 5.0 (Dir 2)	C3011.002a
Ceramic tile floors	SF per 1 gsf	0.028			No Fragility Available
Ceramic tile walls	100 LF per 1 gsf	5.0E-05	14000X0.58 (Dir 1) 14000X0.42 (Dir 2)	0.41 (Dir 1) 0.29 (Dir 2)	C3011.002a
Ceiling - Lay in tile percentage	%	85%	14000/2500	5.6	C3032.002d
Ceiling - Gypsum board percentage	%	5%			No Fragility Available
Ceiling - Exposed percentage	%	8%			No Fragility Available
Ceiling - Other (high end) percentage	%	2%			No Fragility Available
Laboratory Casework	LF per 1 gsf	2.2E-02			No Fragility Available
Fume Hoods	EA per 1 gsf	9.0E-04			No Fragility Available
Stairs	FL per 1 gsf	1.0E-04			No Fragility Available
Elevators	EA per 1 gsf	1.7E-05	14000X8	2	D1014.010
Plumbing Fixtures (Domestic)	EA per 1 gsf	7.0E-04			No Fragility Available
Plumbing Fixtures (Lab)	EA per 1 gsf	2.7E-04			No Fragility Available
Piping: Cold Domestic Water Piping - 2 ½ inch diameter or smaller	1,000 LF per 1 gsf	6.0E-05	14000	0.84	D2021.012a

Table 1-1 Performance Group Calculations for Building A (continued)

Normative Quantity Type	Unit of Measurement	50% Quantity	Measurement for Bldg. A	Quantity for Bldg. A	PACT Perf. Group
Piping: Cold Domestic Water Piping – greater than 2 ½ diameter	1,000 LF per 1 gsf	2.0E-05	14000	0.28	D2021.012a
Piping: Hot Domestic Water Piping - 2 ½ inch diameter or smaller	1,000 LF per 1 gsf	1.2E-04	14000	1.68	D3044.012a
Piping: Hot Domestic Waster Piping – greater than 2 ½ diameter	1,000 LF per 1 gsf	4.0E-05	14000	0.56	D3044.023a
Piping: Gas supply piping	1,000 LF per 1 gsf	1.0E-05			No Fragility Available
Piping: Sanitary Waste Piping	1,000 LF per 1 gsf	8.0E-05	14000	1.12	D2031.012 b
Piping: Process Piping - 2 ½ inch diameter or smaller	1,000 LF per 1 gsf	4.0E-04			No Fragility Available
Piping: Process Piping – greater than 2 ½ diameter	1,000 LF per 1 gsf	1.5E-04			No Fragility Available
Piping: Acid Waste Piping	1,000 LF per 1 gsf	1.5E-04	14000	2.10	D2031.012 b
HVAC: Chiller capacity	TN per 1 gsf	3.3E-03	14000X8	2	D3031.013f
HVAC: Cooling Tower capacity	TN per 1 gsf	3.3E-03	14000X8	2	D3031.023f
HVAC: Boiler capacity	BTU per 1 gsf	65.000			No Fragility Available
HVAC: Air Handling Units	CFM per 1 gsf	1.250	14000X8	5	D3052.013L
HVAC: Fans	CFM per 1 gsf	1.250		0	
HVAC Ducts – 6 sq. feet for larger	1,000 LF per 1 gsf	5.0E-05	14000	0.7	D3041.012 b
HVAC Ducts – less than 6 sq. feet	1,000 LF per 1 gsf	1.0E-04	14000	1.4	D3041.011 b
HVAC in-line Drops & Diffusers	EA per 1 gsf	1.6E-02	14000	22.4	D3041.031 b
HVAC in-line Coils	EA per 1 gsf	2.0E-03			No Fragility Available
HVAC: VAV Boxes	EA per 1 gsf	3.0E-04	14000	4.2	D3041.041 b
Pressure Dependent Air Valves (Phoenix type boxes)	EA per 1 gsf	1.0E-02			No Fragility Available

Table 1-1 Performance Group Calculations for Building A (continued)

Normative Quantity Type	Unit of Measurement	50% Quantity	Measurement for Bldg. A	Quantity for Bldg. A	PACT Perf. Group
HVAC: Steam & Chilled Water Piping - 2 ½ inch diameter or smaller	1,000 LF per 1 gsf	1.0E-05	14000	0.14	D3043.012a
HVAC: Steam & Chilled Water Piping – greater than 2 ½ diameter	1,000 LF per 1 gsf	2.0E-05	14000	0.25	D3043.022a
HVAC: Heating Water Piping - 2 ½ inch diameter or smaller	1,000 LF per 1 gsf	8.0E-05	14000	1.12	D3044.012a
Heating Water Piping – greater than 2 ½ diameter	1,000 LF per 1 gsf	3.0E-05	14000	0.42	D3044.022a
Electrical Load	W per 1 gsf	22.800			No Fragility Available
Electrical Distribution conduits	LF per 1 gsf	5.0E-01			No Fragility Available
Electrical Distribution – cable trays	LF per 1 gsf	4.0E-02			No Fragility Available
Electrical: Wall mounted switchgear	EA per 1 gsf	3.0E-03			No Fragility Available
Electrical: Lighting Fixtures – Lay in fluorescent	EA per 1 gsf	1.5E-02			No Fragility Available
Electrical: Lighting Fixtures – Stem hung fluorescent	EA per 1 gsf	1.5E-02		420	C3034.002
Electrical: Standby generators	KVA per 1 gsf	5.0E-03			No Fragility Available
Fire Protection: Sprinkler Piping	20 LF per 1 gsf	1.0E-02	14000	2.8	D4011.012a
Fire Protection: Sprinkler Drops	EA per 1 gsf	1.0E-02	14000	1.4	D4011.032a

Table 1-2 shows the quantities for the performance groups representing the structural components. As seen in Table 1-2, the cost of structural components is divided among column base plates, column splices, and the connections. We divided the quantities evenly between two directions whenever there was no clear reason on how to distribute the quantities. For instance, Column Base Plates are directional performance groups and we have 40 of such performance groups in Building A. We assumed 20 in Dir 1 and 20 in Dir 2.

Table 1-2 Core & Shell Calculations for Building A

Normative Quantity Type	Unit of Measurement	Measurement for Bldg. A	Quantity for Bldg. A	PACT Perf. Group
Column Base Plates	EA	Based on perimeter number of columns	20 (Dir 1) 20 (Dir 2)	B1031.011b
Column Splices	EA	In stories 3, 5, and 7	20 (Dir 1) 20 (Dir 2)	B1031.021b
Shear Tab Connections	EA	Gravity Columns	28 (Dir 1) 24 (Dir 2)	B1031.001
RBS Connections (two sided)	EA	SMRF	4 (Dir 1) 4 (Dir 2)	B1035.011
RBS Connections (one sided)	EA	SMRF	4 (Dir 1) 4 (Dir 2)	B1035.001

1.1.3.5 Collapse Fragility Tab

The Collapse Fragility tab is where information about the collapse fragility curve of Building A is input. We have used the collapse fragility curve obtained for Building A using the FEMA P695 methodology in which a set of 44 ground motions are applied to building models and scaled up till half of the set (i.e., 22 motions) cause lateral instability (i.e., collapse). Using FEMA P695 methodology the median value of spectral acceleration at the first mode period of Building A was obtained to be 0.29g with a record-to-record variability of 0.4. We considered a $\beta_c = \beta_q = 0.25$ that resulted in total modeling uncertainty of $\beta_M = 0.35$. The value input in the field labeled with “Dispersion” in this tab should contain the total variability in collapse assessment, therefore, we used a value of 0.53 that is the SRSS of the record-to-record variability and modeling uncertainty ($[0.4^2 + 0.35^2]^{0.5} = 0.53$). We assumed collapse happens in a single mode, therefore, the fraction of floors subjected to collapse debris were set to unity. Figure 1-4 shows the information input in PACT Building Manager for Building A.

Pact 2 Building Manager - 8-story Laboratory Building in Sacramento

File Edit Tools Help

Project Info | Building Info | Population | Fragilities | Performance Groups | Collapse Fragility | Structural Analysis

☒ Include Potential Collapse in Assessment

Collapse Fragility Median: Dispersion:

In terms of $S_a(T1)$

Number of Potential Collapse Modes:

Mutually Exclusive Probability of Mode Given Collapse

Mode 1
1

Fraction of Floor Subject to Collapse Debris

Level	Mode 1
Floor 8 (8)	1
Floor 7 (7)	1
Floor 6 (6)	1
Floor 5 (5)	1
Floor 4 (4)	1
Floor 3 (3)	1
Floor 2 (2)	1
Floor 1 (1)	1

Collapse Consequences

Mode 1 of 1

Level	Fatality Rate Mean	Fatality Rate COV	Injury Rate Mean	Injury Rate COV
Floor 8 (8)	0.9	0.0001	0.1	0.0001
Floor 7 (7)	0.9	0.0001	0.1	0.0001
Floor 6 (6)	0.9	0.0001	0.1	0.0001
Floor 5 (5)	0.9	0.0001	0.1	0.0001
Floor 4 (4)	0.9	0.0001	0.1	0.0001
Floor 3 (3)	0.9	0.0001	0.1	0.0001
Floor 2 (2)	0.9	0.0001	0.1	0.0001
Floor 1 (1)	0.9	0.0001	0.1	0.0001

Figure 1-4. PACT input in “Collapse Fragility” tab for Building A

An alternative method for estimating the collapse fragility curve of a building is to use the information obtained from the nonlinear response history analysis at the eight hazard levels used in the time-based loss estimation (see next section). At each hazard level, the number of collapse cases are counted and divided by the total number of ground motion used for loss estimation in that hazard level. The result of this process is the probability of collapse at few hazard levels. Using the maximum likelihood method one can fit a lognormal distribution to this data and obtain the median and aleatory dispersion in the collapse fragility curve. The epistemic variability in estimation of collapse fragility curve can be added to the aleatory one using a SRSS approach where the total dispersion of the collapse fragility curve is inflated.

1.1.3.6 Structural Analysis Results Tab

According to ATC-58 time-based methodology for estimation of losses in buildings, it is required to perform nonlinear response history analysis for

eight levels of seismic hazard. At each hazard level, a set of representative ground motions are selected and applied to the building model; two EDPs in two orthogonal direction are obtained from this analyses. The EDPs of interest for Building A are maximum interstory drift ratio and peak floor acceleration. The aforementioned EDPs are input to PACT Building Manager. Directional EDPs are used to estimate damages and losses to directional performance groups. For non directional performance groups, the program takes the maximum of the corresponding directional EDPs and multiplies this maximum value by a user input value in the field labeled “Non-directional conversion factor;” we assumed a value of 1.2. This means, for instance, that the non directional peak floor acceleration in the second floor is 1.2 times the maximum peak floor acceleration of two orthogonal directions at the second floor. Figure 1-5 shows input to PACT Building Manager for Building A at the first intensity level, for interstory drift ratio affecting direction 1. A set of 11 ground motions was used in this example. We considered a $\beta_c = \beta_q = 0.25$ that resulted in total modeling uncertainty of $\beta_M = 0.35$.

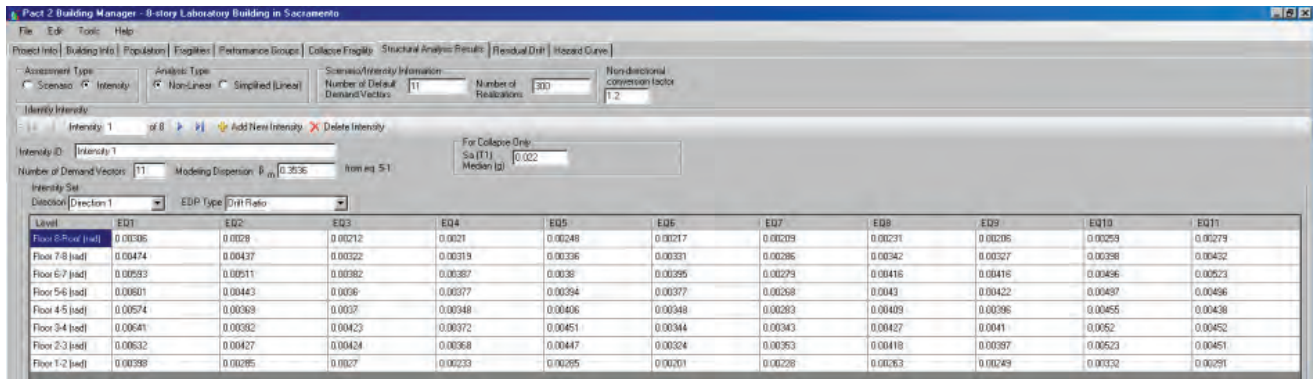


Figure 1-5. PACT input in “Structural Analysis Results” tab for Building A [11 demand vectors, Drift Ratio in Direction 1, First Intensity Measure]

1.1.3.7 Residual Drift Tab

Estimation of losses in buildings can be heavily affected once residual drift is considered in the loss estimation methodology. In the Residual Drift tab, information on demand and capacity for residual drift is input by the user. As for the capacity, we considered using the default value in PACT: median of 1% with dispersion of 30%. The demand values for drift is input by the user; one value for each observation (i.e., each of the eleven analysis) for eight levels of seismic hazard. The calculation of residual drift is based on the procedure outlined in Section 5.4 of guidelines. For Building A, $\Delta_y = 0.01$, and residual drift demand values for each analysis is estimated using Equation 5-20 of the guidelines assuming Δ is the maximum interstory drift along the height of the building.

1.1.3.8 Hazard Curve tab

The last tab in Building Manager is Hazard Curve where information about the hazard for the eight points used in the time-based loss estimation is input. Figure 1-16 shows this tab for Building A. Information for this tab is obtained from the ground motion selection and scaling procedure described in the PACT Beta Test Overview Report, BD-3.7.13.

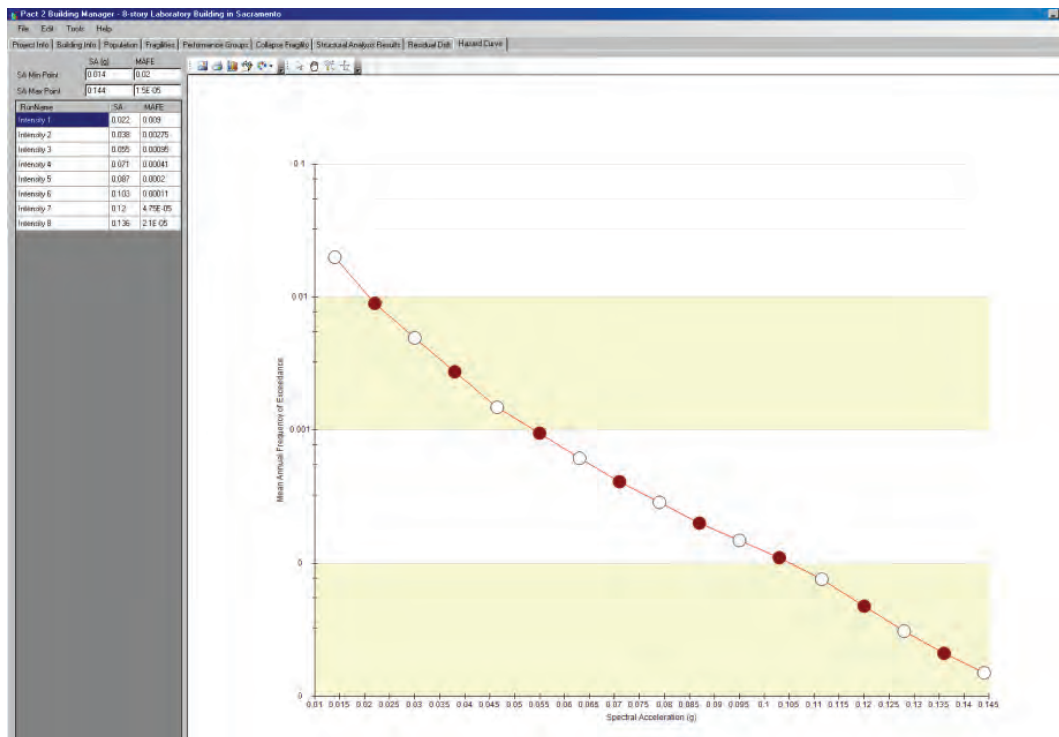


Figure 1-16 PACT input in “Hazard Curve” tab for Building A

1.1.4 Sensitivity of Loss Predictions to Variation in Loss Estimation Parameters.

The intention of this study is to assess the sensitivity of estimated losses to various parameters used in the loss estimation process. The approach we utilized here is to estimate baseline losses for building A considering a set of ideal values for the parameters used in the loss estimation process, A base case. Then, we assess the variation in baseline estimate losses due to variation in parameters of the base case. The baseline loss values for base case Building A is obtained using the following set of parameters:

1. Detailed Analysis Method,
2. 8 stripes on the hazard curve,
3. 11 demand vectors as observations,

4. 300 realizations,
5. Performance group damages are fully correlated.
6. Building Occupancy is “Research”
7. Building is designed for Seismic Design Category of D_{\min} .
8. Modeling uncertainty (β_M) is set to 0.35. $\beta_M = (\beta_c^2 + \beta_q^2)^{0.5} = (0.25^2 + 0.25^2)^{0.5} = 0.35$.
9. Median of residual drift capacity is 1% with associated dispersion of 0.3.
10. Collapse capacity is obtained according to a previous study on Building A.
11. Complete collapse is the single collapse mode. 1.0 debris ratio for all stories, 0.9 fatality rate, 0.1 injury rate. c.o.v. is set to 0.0

For the purpose of this sensitivity study, we looked at probabilistic representation of losses obtained from bins of data rather than a fitted lognormal distribution to the data. At each hazard level, we studied losses associated with 10%, 50% (median), and 90% probability of exceeding. Equations 1-1 to 1-3 show how we obtained the aforementioned quantities. In these equations, \mathbf{L} is a sorted vector of loss values obtained from loss estimation (i.e., Repair Cost, Repair Time) and has r number of realizations (e.g., $r = 300$ for 300 realizations), *round* is a function that rounds a number to first digit.

$$10\% \text{ loss}_{\text{bins}} = \mathbf{L} \left(\text{round} \left(\frac{r}{10} \right) \right) \quad (1-1)$$

$$50\% \text{ loss}_{\text{bins}} = \frac{1}{2} \left[\mathbf{L} \left(\text{round} \left(\frac{r}{2} \right) - 1 \right) + \mathbf{L} \left(\text{round} \left(\frac{r}{2} \right) \right) \right] \quad (1-2)$$

$$90\% \text{ loss}_{\text{bins}} = \mathbf{L} \left(\text{round} \left(\frac{r}{90} \right) \right) \quad (1-3)$$

1.1.4.1 Sensitivity of Loss Predictions to Variation in Number of Realizations

Identifying the minimum number of realization by which a stable estimate of loss is achieved was the first problem we addressed. Small number of realizations can potentially lead to an incorrect estimate of loss, rendering the whole loss estimation exercise unreliable. In theory, as the number of realizations in the loss estimation process grows, the estimated losses converge to robust values. In this section we show the process employed for identifying the optimum number of realizations for loss estimation of the

base case for Building A. We found this optimum value for Building A to be 200, however, we have use a number equal to 300 in the rest of this study to assure convergence of losses for cases other than the base case.

Given the large number of stories for Building A, we were unable to successfully run PACT and save analysis results once number of realizations was more than 300. We tried to overcome with shortcoming with a brute force approach, that is, we ran PACT with 300 realizations more than once and combined loss realizations. We considered running PACT for the base case 20 times, with seed number equal to zero, and save estimated loss values for each realization. Given the procedure by which PACT estimates losses at each target hazard, one can argue that the ensemble of estimated losses from all 20 PACT runs (total of $20 \times 300 = 6000$) is statistically similar to a single PACT run with 6000 realizations. We generated this ensemble and claim that the estimated distribution of loss from 6000 realizations is a robust estimate of true loss distribution.

PACT uses the distribution function of loss at each target hazard to report corresponding statistical measures of loss (e.g., median of loss at target hazard level), as well as annualized losses. Therefore, one can claim that the optimum number of realizations is the one that can generate a distribution function of loss similar enough to the same distribution function obtained from 6000 realizations. The similarity between two loss distribution functions is measured by the Kolmogorov-Smirnov test. Using this test, we show that the estimated distribution of loss with 300 realizations is statistically similar to the one obtained from 6000 realizations. Figure 1-17 shows this process for one of the hazard levels for Building A, similar results are obtained for other hazards. The upper and lower parts of Figure 1-17 show distribution functions for repair cost and repair time, respectively, for the base case at one of the hazard levels (similar results are obtained for other hazard levels of the base case). In each plot, the distribution function shown with black solid line is the one obtained using 6000 realizations, the dash lines show the upper and lower bound for any other distribution function with smaller number of realizations that satisfy the Kolmogorov-Smirnov test for 5% significance. The left hand side of Figure 1-17 is dedicated to investigate if 100 realizations are enough for providing an acceptable estimate of loss distribution function, and the right hand side to 300 realizations for the same purpose. The red thin lines show the distribution functions that we obtained using subsets of 100 realizations (for the left hand side plots) and 300 realizations (for the right hand side plots). We drew 40 sets of 100, or 300, realizations from the original 6000 realizations; hence, 40 distribution functions are shown with 40 red color curves. Investigation of

the left hand side of Figure 1-17 shows that using 100 realizations can lead to estimates of loss distribution function that fails the Kolmogorov-Smirnov test, however, using 300 realizations provides an acceptable distribution function for loss.

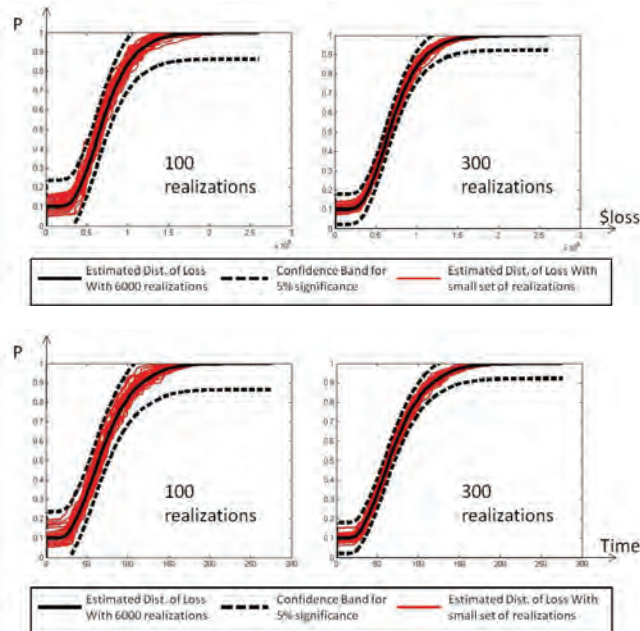


Figure 1-17 Distribution of loss at the first hazard level.

1.1.4.2 Sensitivity of loss predictions to variation in modeling uncertainty β_m .

Effect of modeling uncertainty is incorporated in the guidelines through variable β_m ; $\beta_m = (\beta_c^2 + \beta_q^2)^{0.5}$, where β_c and β_q are element modeling, and element hysteretic models uncertainty. For the base case, we assumed β_c and β_q are equal to 0.25 leading to $\beta_m = 0.35$. In this sensitivity analysis, we will look into two cases: $\beta_m = 2 \times 0.35 = 0.70$, and $\beta_m = 0.5 \times 0.35 = 0.18$.

The value of β_m is directly used in the Structural Analysis Results tab, however, extra care should be given to Collapse Fragility Tab. In the later, the input to the field labeled “Dispersion,” is the record-to-record variability of the collapse fragility curve inflated by the variability due to modeling uncertainty. In the base case, total dispersion of the collapse fragility curve is set to $0.53 = (0.4^2 + 0.35^2)^{0.5}$; 0.4 is the record-to-record variability in collapse fragility curve, and 0.35 is the modeling uncertainty. For cases that we set modeling uncertainty, β_m , to 0.70 and 0.18, the total dispersion of the collapse fragility curve is set to $0.81 = (0.4^2 + 0.70^2)^{0.5}$, and $0.44 = (0.4^2 + 0.18^2)^{0.5}$, respectively.

Variation in modeling uncertainty has a negligible effect on estimate of median of loss. This shows that variation in modeling uncertainty, β_m , does not generate much bias in estimates of loss. Figures 1-18 and 1-19 show the sensitivity of median of repair cost, and repair time, to variation of β_m . These figures show the median estimate losses for the 8 hazard levels considered in this study.

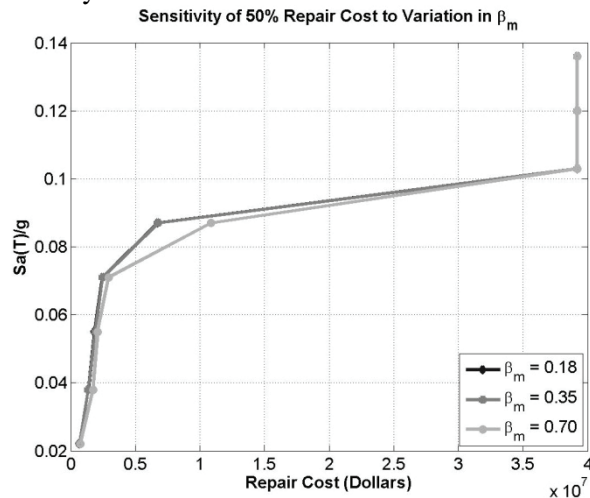


Figure 1-18 Median Repair Cost curve estimated for variation in β_m

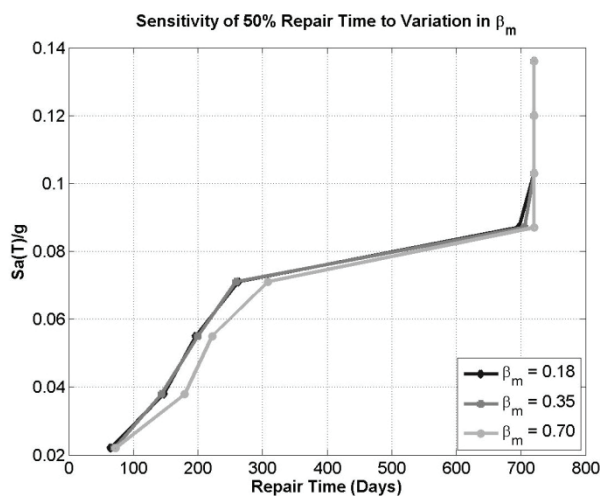


Figure 1-19 Median Repair Time curve estimated for variation in β_m

Variation in β_m has some effect on 10% and 90% fractiles of estimated repair cost and repair time. Although the median estimate of each loss is not much affected by variation of β_m , but variability in estimated losses is affected. Figures 1-20 & 1-21 show the 90% loss estimates and Figures 1-22 & 1-23 show the 10% estimates. Investigation of these figures show that the 90% estimate of loss is larger for larger β_m , and 10% estimates of loss is smaller

for larger β_m . This trend clearly shows a larger variability in estimation of loss once larger value of β_m is employed.

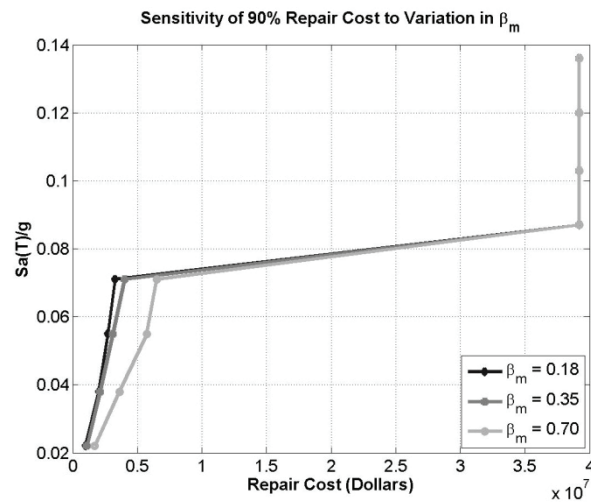


Figure 1-20 90% Repair Cost curve estimated for variation in β_m

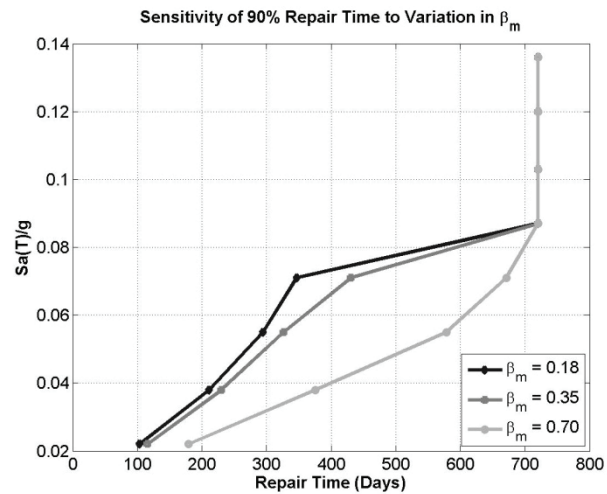


Figure 1-21 90% Repair Time curve estimated for variation in β_m

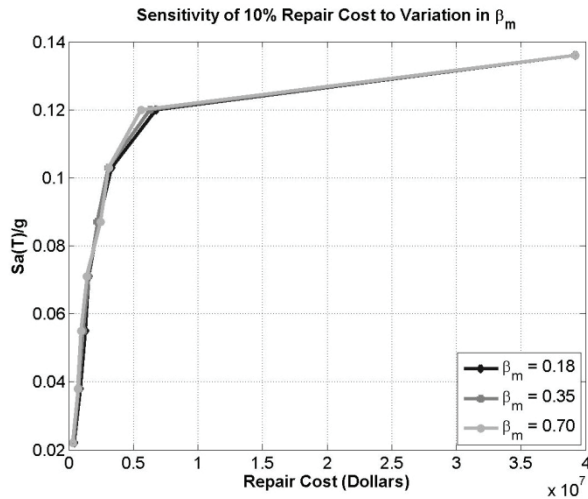


Figure 1-22 10% Repair Cost curve estimated for variation in β_m

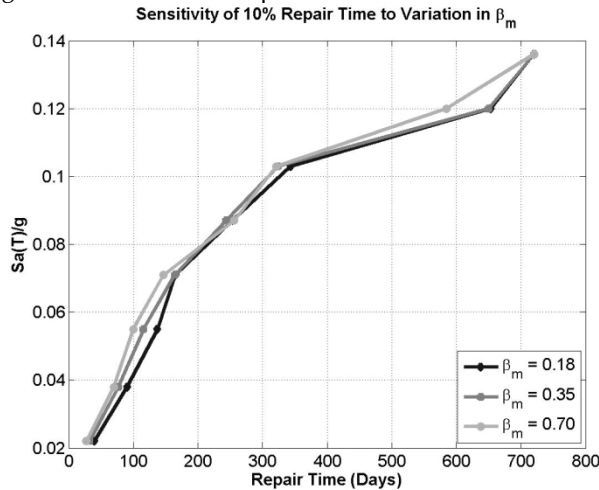


Figure 1-23 10% Repair Time curve estimated for variation in β_m

Table 1-3 shows the variation in annualized loss estimates for variation in β_m . It is not surprising to see larger estimates of loss for larger values of β_m . Increase in β_m results in larger variability in estimates of loss per hazard level. Consequently, integration of distribution of loss with larger dispersion per hazard level over the entire length of the hazard curve results in larger estimates of annualized loss.

Table 1-3 Variation in Estimated Annualized Loss to Variation in β_m				
Case	Annualized Repair Cost	Annualized Repair Time	MAF. of Collapse	MAF of Red Tag
$\beta_m = 0.35$ (Base Case)	\$26,573	0.58 Days	7.427 E-6	5.333 E-4
$\beta_m = 0.70$	\$30,951	0.67 Days	10.7 E-6	5.818 E-4
$\beta_m = 0.18$	\$23,394	0.52 Days	0.850 E-6	2.806 E-4

1.1.4.3 Sensitivity of Loss Predictions to Variation in Median Collapse Capacity Sa_C .

We investigated the variability in losses due variation in median collapse capacity, Sa_C . The median collapse capacity is a spectral acceleration at the fundamental period of the structure where probability of collapse is 50%. For the base case, we obtained $Sa_C = 0.29g$ from an independent analysis using FEMA P695 approach.

We did not use the results of nonlinear response history analyses obtained from using the ground motions associate with the 8 stripes considered in this study. We did not see any collapse cases in any of the analyses, therefore, could not fit a probability distribution function to collapse cases and obtain Sa_C . Ideally, results tabulated in Structural Analysis tab and Collapse Fragility tab should come from a unique set of analysis.

Two alternatives for Sa_C was considered; $Sa_C = 0.14g$ and $Sa_C = 0.11g$. These two values correspond to 10% and 20% probability of collapse at the 2% in 50 years hazard level (assuming the same dispersion in collapse fragility and equal to 0.53). $Sa_C = 0.29$, the value of median collapse capacity for the base case, will result in 0.4% probability of collapse at the 2% in 50 years hazard level.

Variation in Sa_C has a relatively small effect on median estimate of losses. It is expected to obtain a smaller estimate of median loss for larger Sa_C values, however, the difference in median loss is not significant. Figures 1-24 and 1-25 show the sensitivity of median of repair cost, and repair time, to variation of Sa_C . These figures show the median estimate losses for the 8 hazard levels considered in this study.

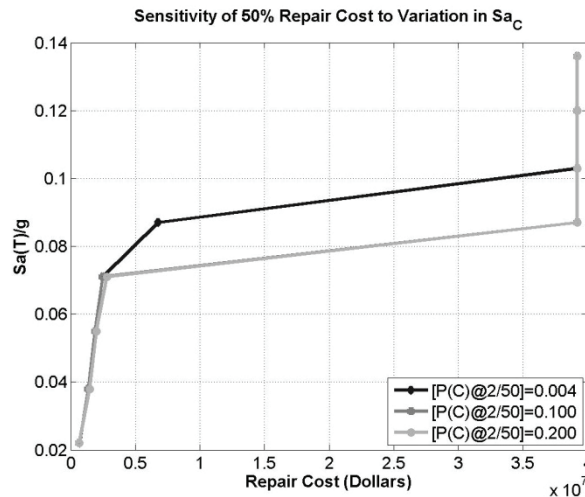


Figure 1-24 Median Repair Cost curve estimated for variation in Sa_C

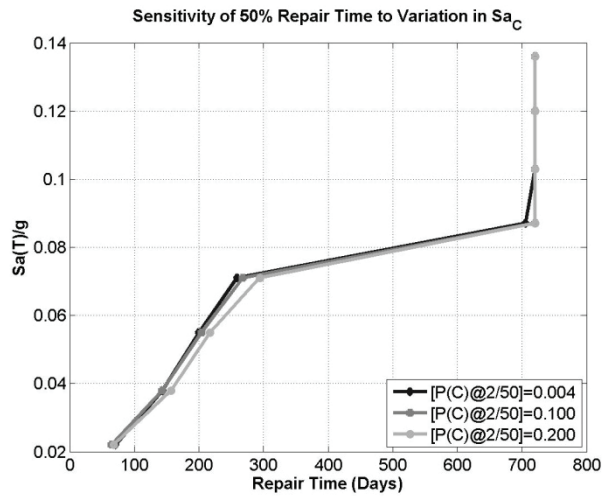


Figure 1-25 Median Repair Time curve estimated for variation in Sa_C

Sa_C has a significant effect on the upper bound, 90% fractile, estimate of losses as shown in Figure 1-26 and 1-27. A smaller value for Sa_C results in abrupt saturation of loss at 90% fractile estimate. Figures 1-28 & 1-29 show the 10% estimates and the difference between estimated losses for various Sa_C values is small.

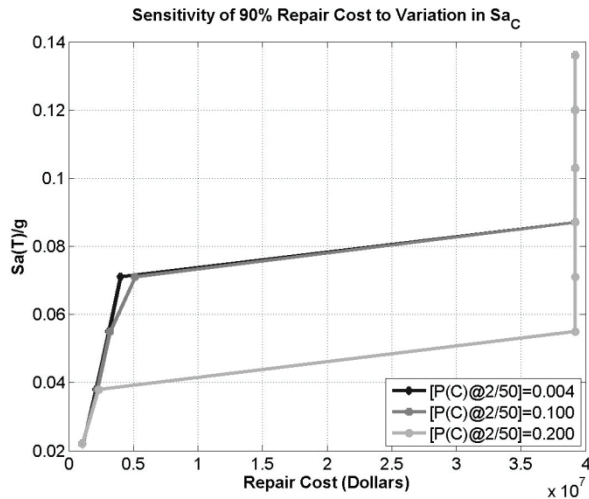


Figure 1-26 90% Repair Cost curve estimated for variation in Sa_C

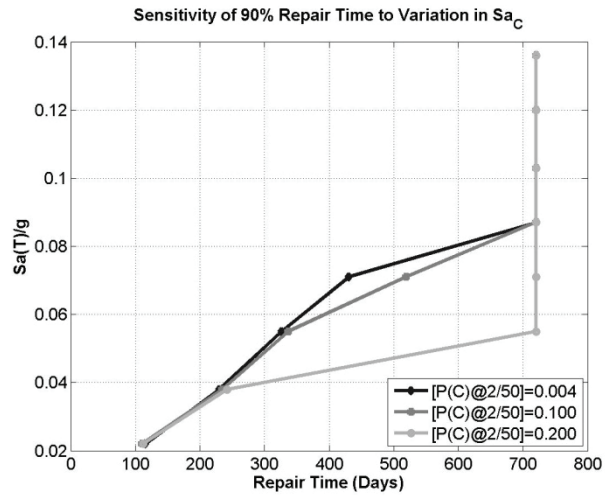


Figure 1-27 90% Repair Time curve estimated for variation in Sa_C

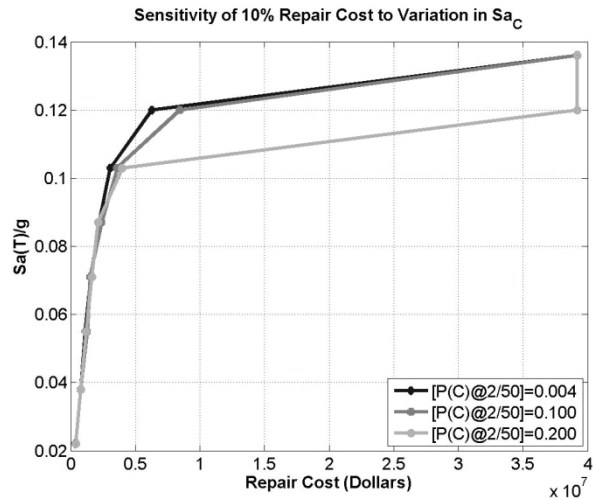


Figure 1-28 10% Repair Cost curve estimated for variation in Sa_C

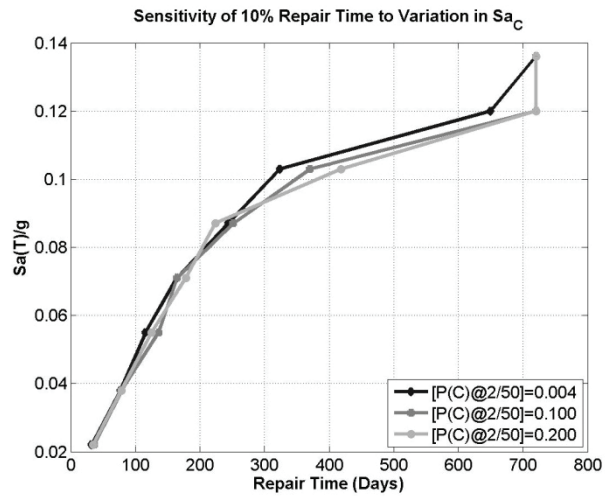


Figure 1-29 10% Repair Time curve estimated for variation in Sa_C

Table 1-4 shows the variation in annualized loss estimates for variation in Sa_C . Increase in MAF of collapse is inevitable once median of collapse capacity is reduced. However, the annualized repair cost and repair time do change significantly only for the case where $Sa_C = 0.11g$. This can be due to small contribution of collapse on annualized loss at low probability hazard levels. Once collapse occurrence is more likely in hazards that have high probability, and consequently high weight in estimation of annualized loss, then a significant change in annualized loss due to reduction in Sa_C is observed.

Case	Annualized Repair Cost	Annualized Repair Time	MAF. of Collapse	MAF of Red Tag
$Sa_C = 0.29g$ (Base Case)	\$26,573	0.58 Days	7.427 E-6	5.333 E-4
$Sa_C = 0.14g$	\$26,369	0.57 Days	17.6 E-6	3.65 E-4
$Sa_C = 0.11g$	\$34,316	0.71 Days	40.0 E-6	5.56 E-4

1.1.4.4 Sensitivity of loss predictions to variation in median residual drift capacity Δ_{res} .

For a building subjected to seismic excitation, a residual drift demand larger than residual drift capacity, denoted as Δ_{res} , can render the building as a complete loss although collapse has not occurred. We have investigated the effect of varying Δ_{res} from PACT default value, 0.01, on losses; we looked into two cases: $\Delta_{res} = 2 \times 0.01 = 0.02$, and $\Delta_{res} = 0.5 \times 0.01 = 0.005$.

Variation in Δ_{res} has a significant effect on estimate of median of loss. Figures 1-30 and 1-31 show the sensitivity of median of repair cost, and repair time, to variation of Δ_{res} for the 8 hazard levels considered in this study. Three observations are of significance in these two figures:

1. At low intensity measures, high probability hazard levels, the effect of variation of residual drift capacity on losses is close to zero. This is due to the behavior of building A in high probability hazard levels in which not much nonlinear action happens and the building is more or less elastic with no residual drift.
2. At high intensity measure, low probability hazard levels, the effect of variation on residual drift capacity is once again negligible. This is due to high seismic demands and saturation of loss to maximum value.
3. There is a zone between the high and low probability hazard levels that higher Δ_{res} can lead to lower losses and visa versa. The extend of this

middle zone on the intensity measure axis is also a function of Δ_{res} ; lower values of residual drift capacity forces the middle zone to shrink.

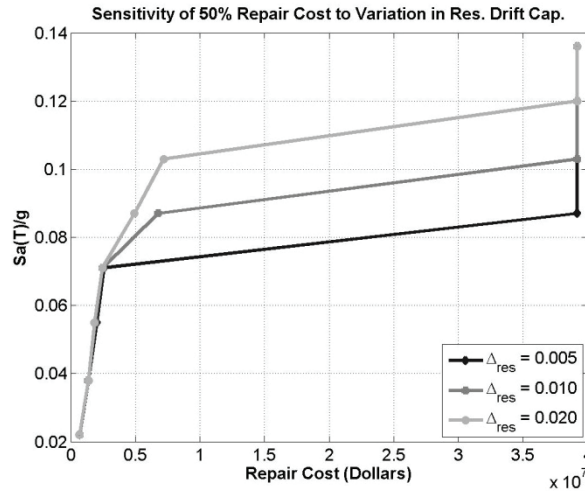


Figure 1-30 Median Repair Cost curve estimated for variation in Δ_{res}

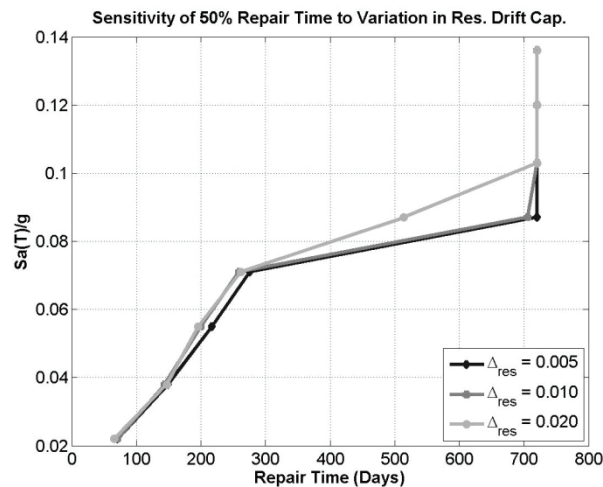


Figure 1-31 Median Repair Time curve estimated for variation in Δ_{res}

The high and low fractiles of loss for various values of Δ_{res} indicate that variability in estimated loss is affected with change in Δ_{res} . Figures 1-32 & 1-33 show the 90% loss estimates and Figures 1-34 & 1-35 show the 10% estimates of loss for values of Δ_{res} considered in this study. These figures show that the 90% estimate of loss for small values of Δ_{res} is at maximum loss value for low and moderate hazard levels. Same observation can be made for higher Δ_{res} values, however, a larger range of hazard remains with a loss less than the maximum loss value.

On the contrary, the 10% estimate of loss shows a clear trend for effect of $\Delta_{res} = 0.005, 0.01, \text{ and } 0.02$; for high probability hazard levels, the estimate

of 10% loss is almost identical. For lower probability hazards, an increase in residual drift capacity results in a reduction of the 10% fractile estimate of, however, this reduction does not necessarily follow the same trend as Δ_{res} .

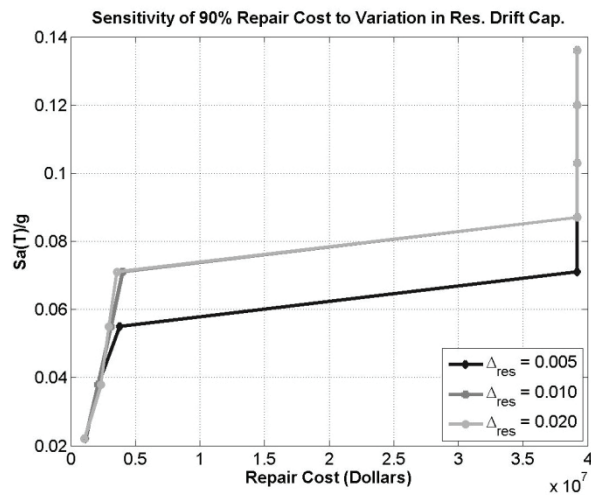


Figure 1-32 90% Repair Cost curve estimated for variation in Δ_{res}

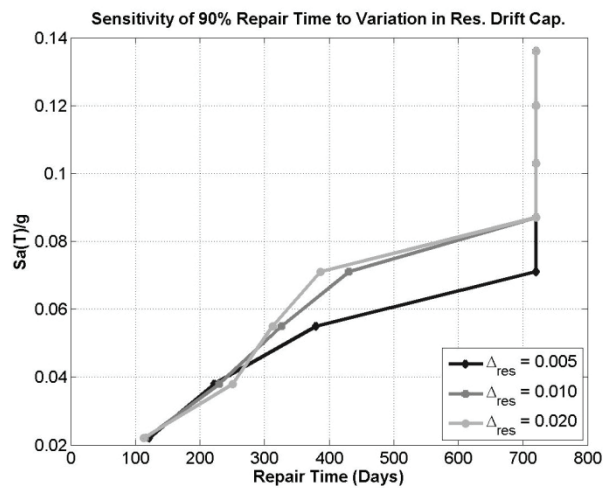


Figure 1-33 90% Repair Time curve estimated for variation in Δ_{res}

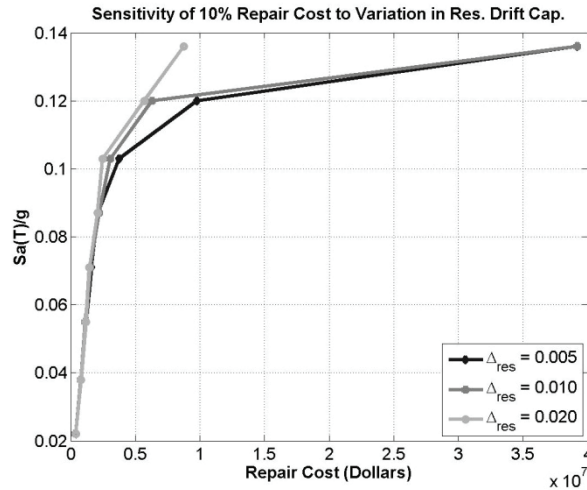


Figure 1-34 10% Repair Cost curve estimated for variation in Δ_{res}

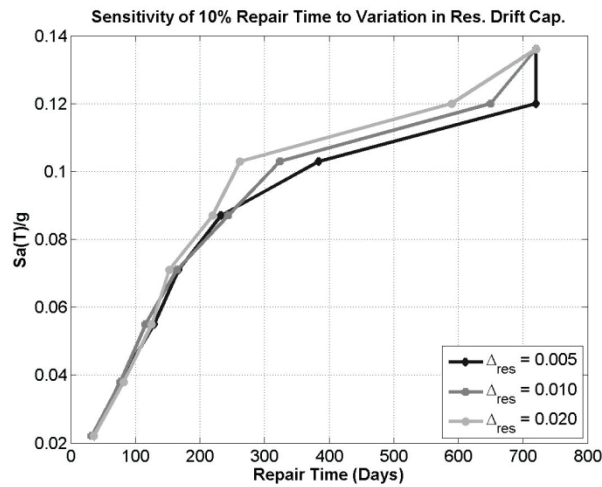


Figure 1-35 10% Repair Time curve estimated for variation in Δ_{res}

Table 1-5 shows the variation in annualized loss estimates for variation in Δ_{res} . We expect to see an increase in annualized repair cost for $\Delta_{res} = 0.005$, and a decrease in repair cost for $\Delta_{res} = 0.2$; this is confirmed by numbers in Table 1-5. To some extent, repair time follows the same trend as repair cost. We are surprised to see the effect Δ_{res} on MAF of collapse; theoretically, collapse is not synonymous with residual drift more than its capacity. It appears that PACT treats cases in which residual drift exceeds its capacity as collapse; therefore, MAF of collapse increases with decrease in Δ_{res} .

Table 1-5 Variation in Estimated Annualized Loss to Variation in Δ_{res}

Case	Annualized Repair Cost	Annualized Repair Time	MAF. of Collapse	MAF of Red Tag
$\Delta_{res} = 0.01$ (Base Case)	\$26,573	0. 58 Days	7.427 E-6	5.333 E-4
$\Delta_{res} = 0.005$	\$27,232	0.58 Days	8.57 E-6	3.604 E-4
$\Delta_{res} = 0.02$	\$20,324	0.46 Days	6.80 E-6	2.192 E-4

1.1.4.5 Sensitivity of loss predictions to variation in number of demand vectors.

To study the sensitivity of losses to number of demand vectors used in the loss estimation process, we considered varying the number of demand vectors from the base case, 11, to: 20, 7, 5, 3. Unfortunately, we were unable to obtain a successful analysis for all cases other than two: cases in which number of demand vectors were equal to 20 and 11. Our investigation shows that the main reason for this lack of success is due to unacceptable pseudo-zero values used in the Residual Drift tab for high probability hazard levels. A value of zero as residual drift demand value will force the program to reject analysis, therefore, a small number, aka pseudo-zero, (e.g., 0.0001) is use in lieu of zero. Once the number of demand vectors is less than 11, PACT will reject analysis, however, it will work if the pseudo-zero demand values in the residual drift tab are set to larger values. A large value for residual drift demand that supposed to be zero will result in erroneous estimate of loss.

Effect of using a larger set of demand vectors would affect the mean and covariance matrix of EDPs used in the loss estimation process. Figures 1-36 1-41 show the 10%, 50%, and 90% fractiles of repair cost and repair time at various hazard levels for the two cases studied here: number of observations equal to 11 and 20. It appears that estimate of median loss does not change radically, unless only at one hazard level (see Figure 1-36 and 1-37). Investigation of other figures show that variability in estimation of loss is larger for the case where 11 observations where used compared to 20 observations. One can argue that for an 8-story building with total of 17 EDPs (8 maximum interstory drifts, 9 peak floor accelerations), a set of 11 observations is not enough to develop a full rank EDP covariance matrix. A set of 20 observation would be marginally enough to provide a full rank EDP covariance matrix.

Table 1-6 shows the variation in annualized loss estimates for two cases studied here. Given the larger variability in estimate of losses at each hazard

for the case where 11 observation EDP vectors were used compared to 20 EDP vectors, the corresponding annualized loss values are larger as well.

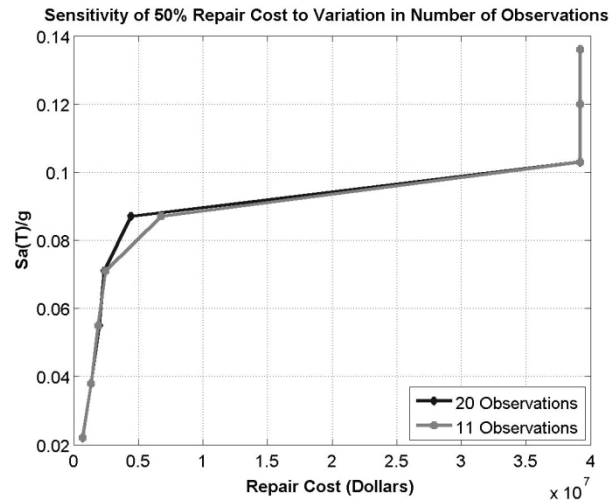


Figure 1-36 Median Repair Cost curve estimated for variation in number of observations

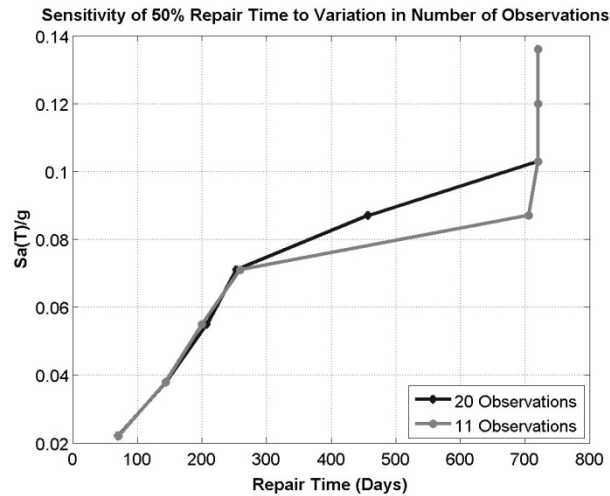


Figure 1-37 Median Repair Time curve estimated for variation in number of observations

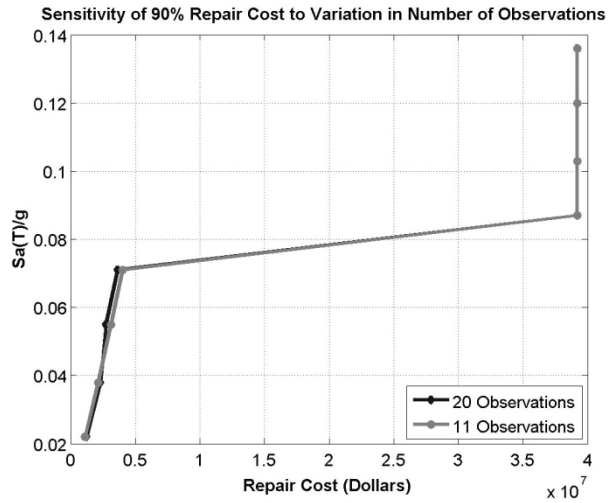


Figure 1-38 90% Repair Cost curve estimated for variation in number of observations

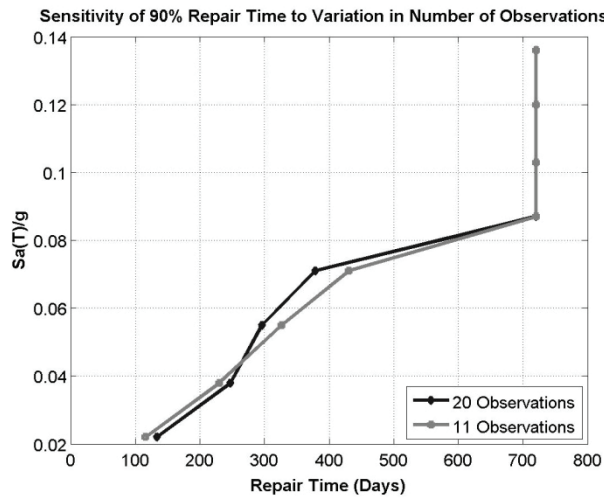


Figure 1-39 90% Repair Time curve estimated for variation in number of observations

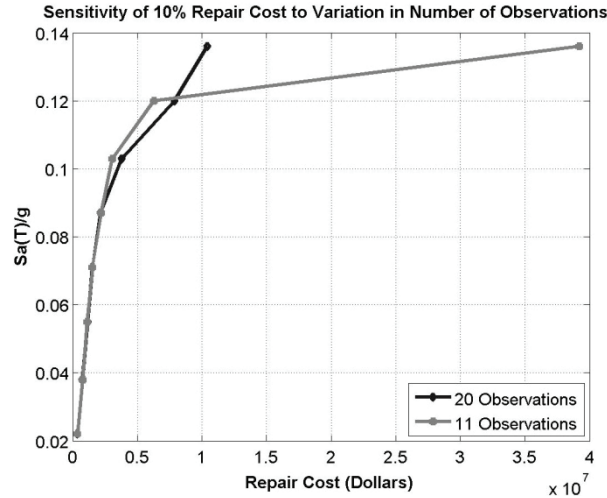


Figure 1-40 10% Repair Cost curve estimated for variation in number of observations

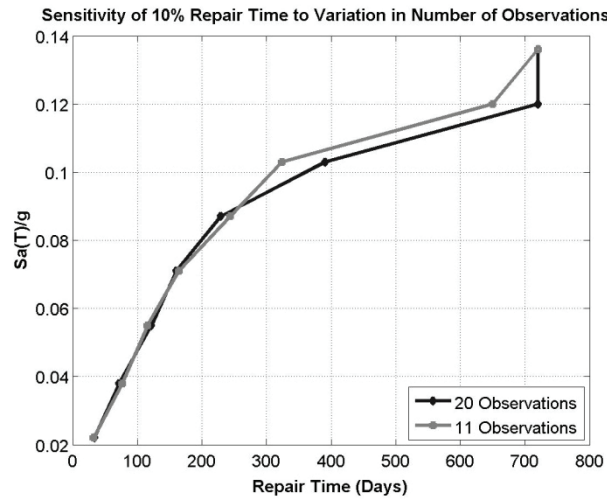


Figure 1-41 10% Repair Time curve estimated for variation in number of observations

Table 1-6 Variation in Estimated Annualized Loss to Variation In Number of Demand Vectors

Case	Annualized Repair Cost	Annualized Repair Time	MAF. of Collapse	MAF of Red Tag
11 Vec. (Base Case)	\$26,573	0.58 Days	7.427 E-6	5.333 E-4
20 Vec.	\$20,967	0.47 Days	11.42 E-6	1.895 E-4

1.1.4.6 Sensitivity of loss predictions to variation in structural design provisions.

We investigated the difference between the estimate of loss for base case Building A with a similar one but stiffer and stronger. This design alternative

was designed for $SDC = D_{\max}$ rather than D_{\min} (the base case). Our analysis shows that losses in a building designed for $SDC = D_{\max}$ can be radically smaller than the same building designed for $SDC = D_{\min}$. Please note that both buildings are located in a location with low seismicity, D_{\min} , and we are applying the same ground motions that we applied to the base case of building A to the design for $SDC = D_{\max}$. It is worth mentioning that the 8-story building designed for $SDC = D_{\max}$ has a fundamental period $T_l = 2.29$ sec., and median of collapse capacity, $Sa_C = 0.73g$ (in contrast, same values for the base are $T_l = 3.55$ sec., and median of collapse capacity, $Sa_C = 0.29g$).

The reduction in period of vibration of the alternative structure is a direct consequence of higher stiffness of its beam and columns. This translates into smaller deformation demand values. At the same time, the collapse capacity is much larger for the alternative design compared to the base case, therefore, we expect that all fractiles of loss, 10% & 50% and 90%, be smaller than the same values for the base case. Figures 1-42 to 1-47 show the variation of fractiles of loss at various hazard levels for two designs.

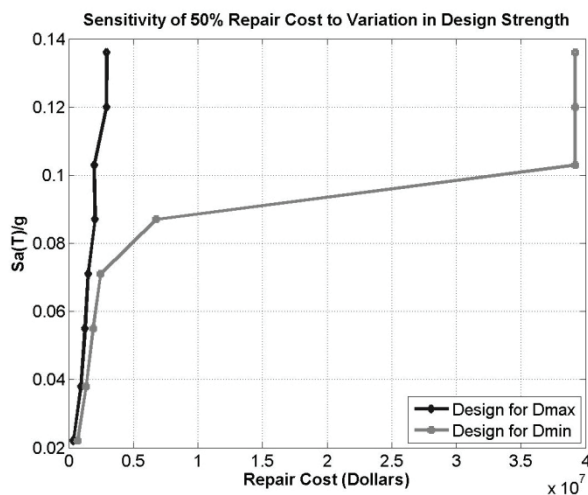


Figure 1-42 Median Repair Cost curve estimated for variation in design strength

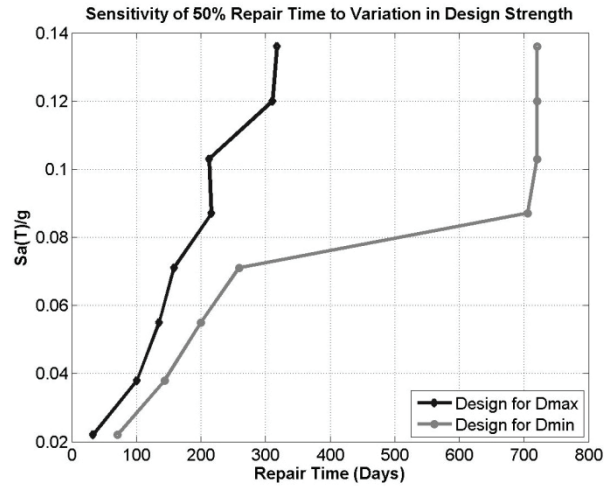


Figure 1-43 Median Repair Time curve estimated for variation in design strength

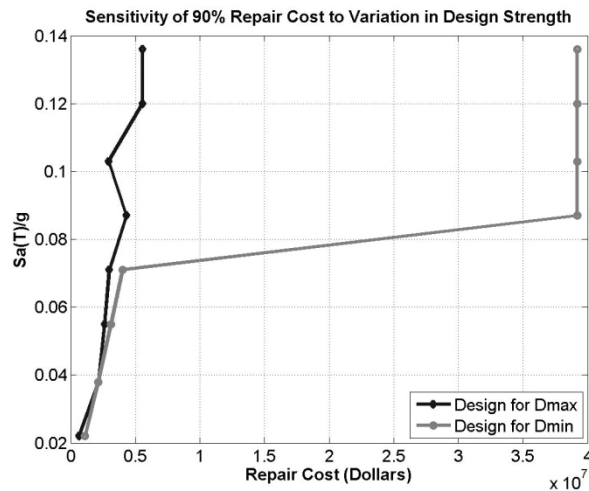


Figure 1-44 90% Repair Cost curve estimated for variation in design strength

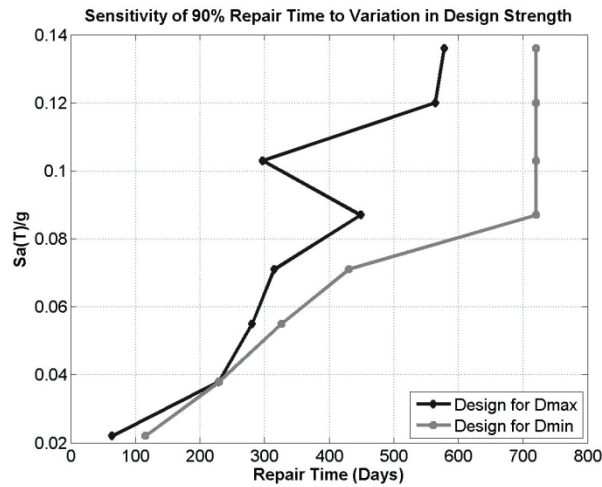


Figure 1-45 90% Repair Time curve estimated for variation in design strength

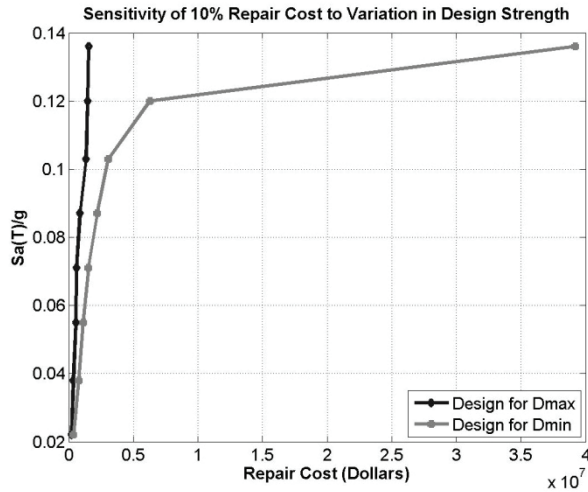


Figure 1-46 10% Repair Cost curve estimated for variation in design strength.

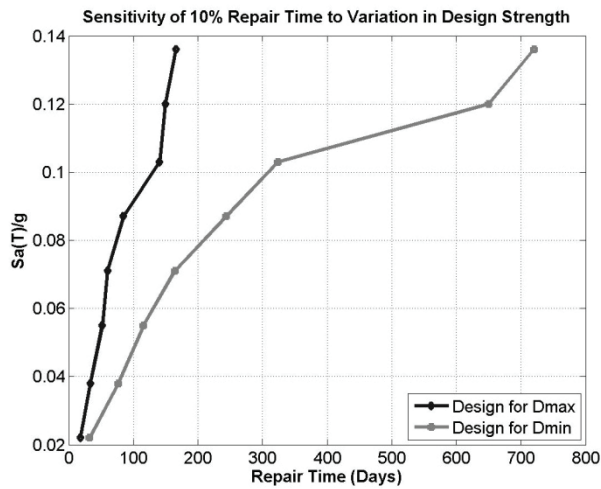


Figure 1-47 10% Repair Time curve estimated for variation in design strength.

Table 1-7 shows the variation in annualized loss estimates for two cases studied here. Given the larger median and variability in estimate of losses at each hazard for the base case compared to the stiffer and stronger design alternative, the corresponding annualized loss values are larger as well.

Table 1-7 Variation in Estimated Annualized Loss to Variation in Structural Design Provisions

Case	Annualized Repair Cost	Annualized Repair Time	MAF. of Collapse	MAF of Red Tag
D_{min} (Base Case)	\$26,573	0.58 Days	7.427 E-6	5.333 E-4
D_{max}	\$10,554	0.26 Days	00.0 E-6	0.884 E-4

1.1.4.7 Sensitivity of loss predictions to variation in building occupancy.

We investigated the effect of variation in building occupancy on losses. Figures 1-48 to 1-53 show the variation of repair cost and repair time for three fractiles of 10%, 50%, and 90%. It not surprising that the losses are not much different as only the occupancy type was changed in the base case PACT model.

We have looked into variation of fatalities and injuries due to variation in building occupancy. Given the low probability of collapse for this building, the rate of fatalities and injuries was almost unchanged among all occupancies. Figures 1-54 to 1-59 show the numbers for these forms of loss.

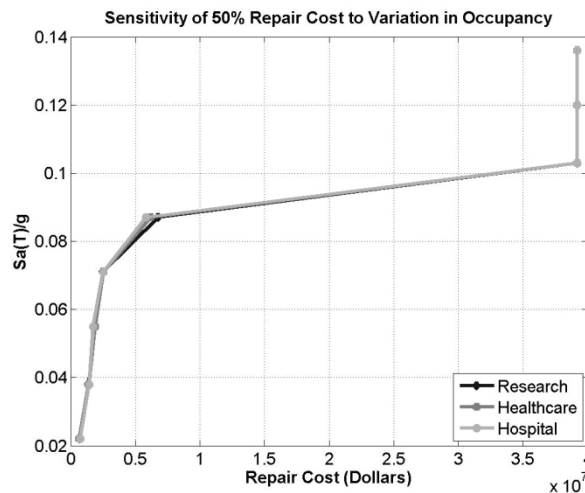


Figure 1-48 Median Repair Cost curve estimated for variation in building occupancy.

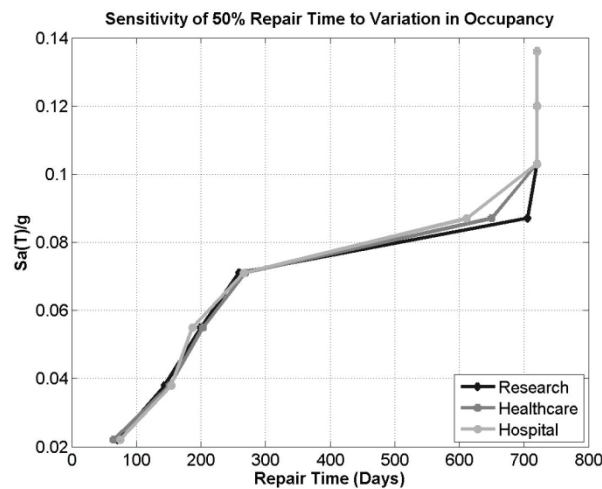


Figure 1-49 Median Repair Time curve estimated for variation in building occupancy.

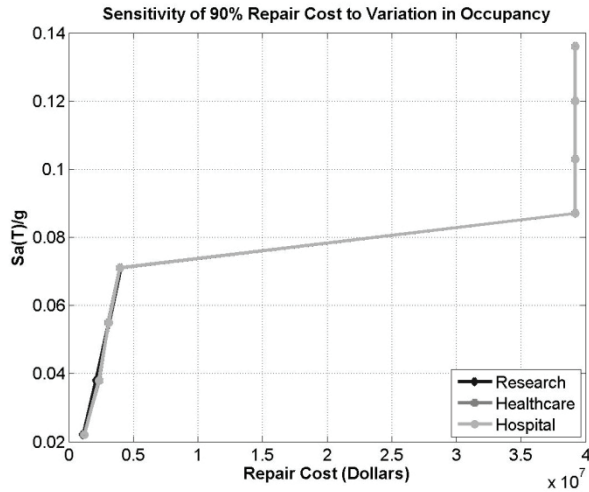


Figure 1-50 90% Repair Cost curve estimated for variation in building occupancy.

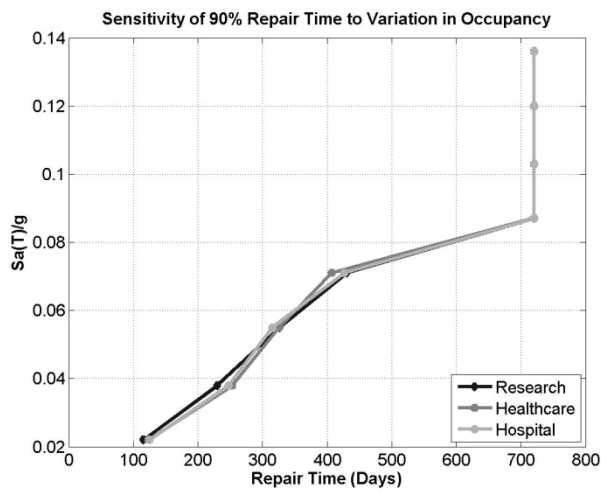


Figure 1-51 90% Repair Time curve estimated for variation in building occupancy.

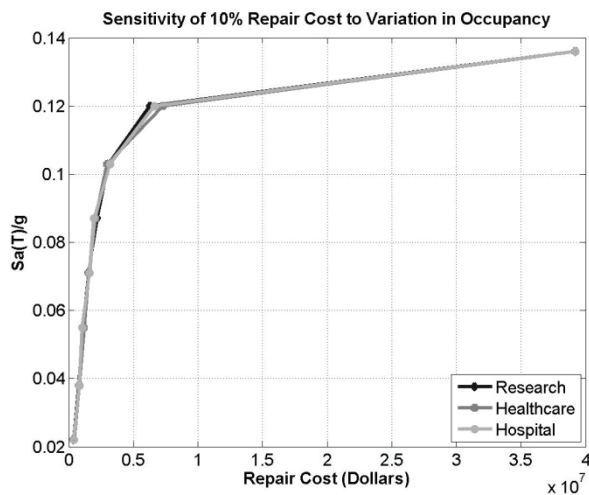


Figure 1-52 10% Repair Cost curve estimated for variation in building occupancy.

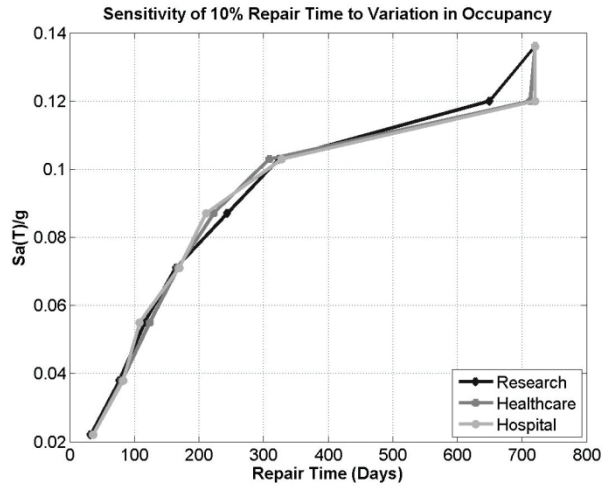


Figure 1-53 10% Repair Time curve estimated for variation in building occupancy

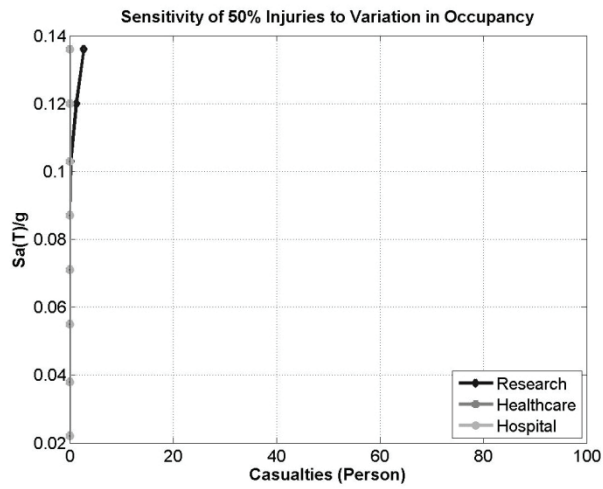


Figure 1-54 Median number of injuries estimated for variation in building occupancy

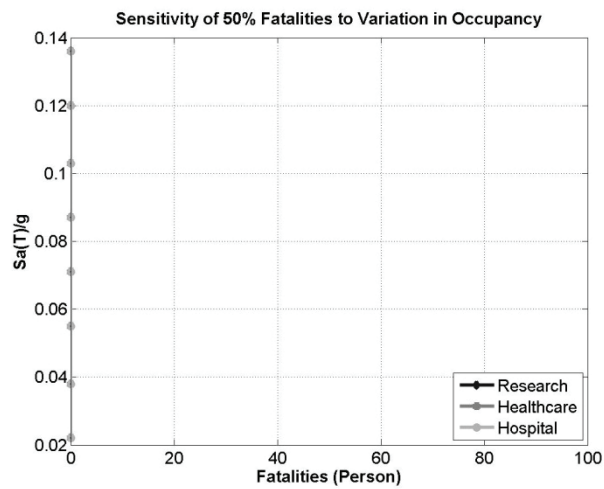


Figure 1-55 Median number of fatalities estimated for variation in building occupancy

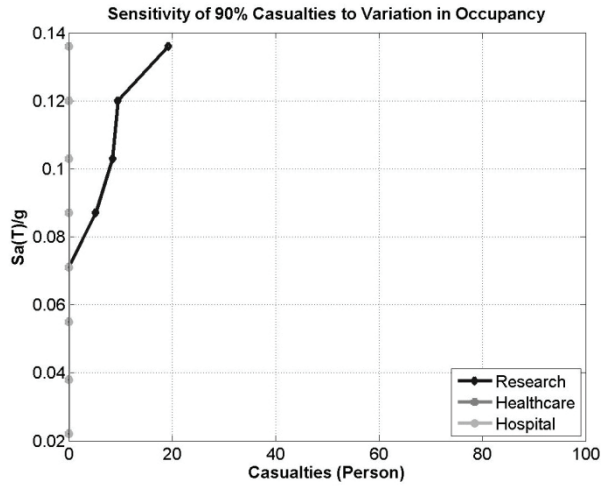


Figure 1-56 90% number of injuries estimated for variation in building occupancy

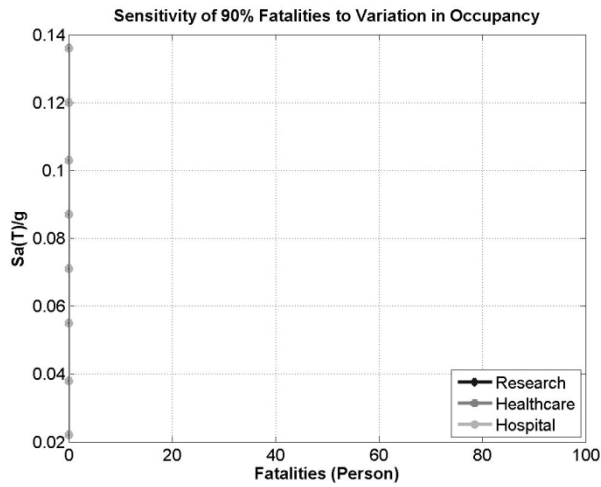


Figure 1-57 90% number of fatalities estimated for variation in building occupancy

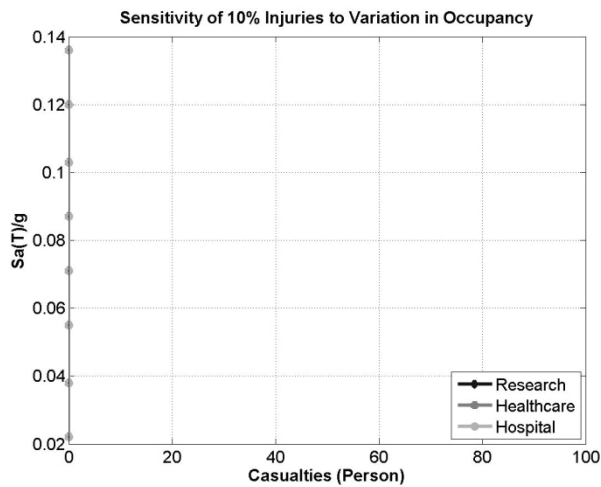


Figure 1-58 10% number of injuries estimated for variation in building occupancy

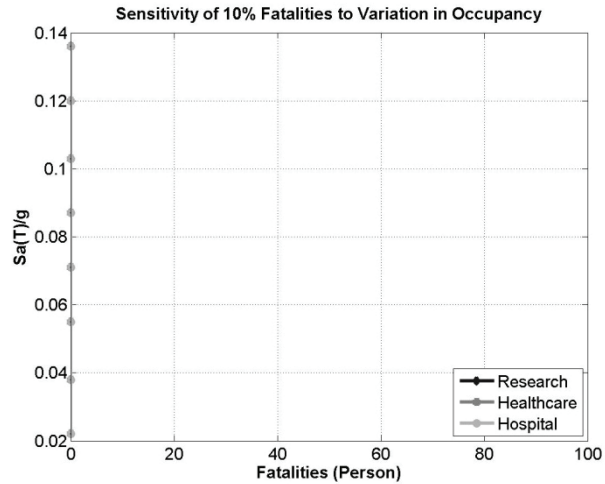


Figure 1-59 10% number of fatalities estimated for variation in building occupancy

Table 1-8. Variation in estimated annualized loss to variation in building occupancy

Case	Annualized Repair Cost	Annualized Repair Time	MAF. of Collapse	MAF of Red Tag
Research (Base Case)	\$26,573	0.58 Days	7.427 E-6	5.333 E-4
Hospital	\$23,002	0.51 Days	12.198 E-6	2.709 E-4
Health Care	\$22,977	0.51 Days	8.607 E-6	2.620 E-4

1.1.4.8 Sensitivity of loss predictions to variation in collapse mode.

We investigated the effects of variation in modes of collapse. Collapse modes affect the fraction of floors subject to collapse debris. We looked into three variation of the base case (that was complete collapse of all floors once building is in collapse state):

Alternative 1: first floor at 90% and other floors at 10%.

Alternative 2: first floor at 90% and other floors at 50%.

Our investigation shows that variation in collapse mode does not affect any form of loss. This is due to small probability of collapse for this building. The repair cost and repair time are essentially the same. Figure 1-60 to Figure 1-65 show variation of fatalities and injuries due to variation in collapse modes.

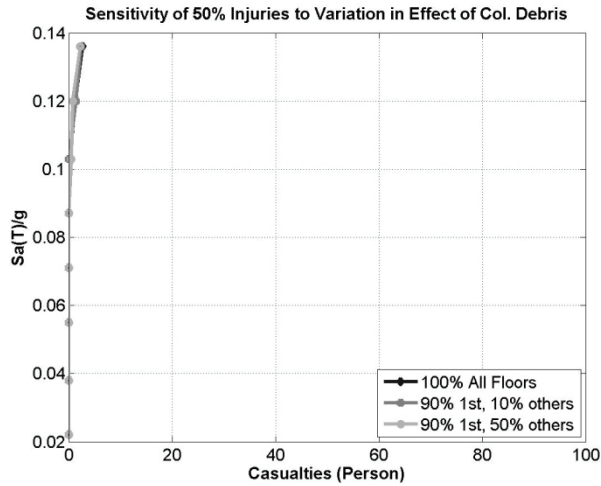


Figure 1-60 Median number of injuries estimated for variation in building collapse mode

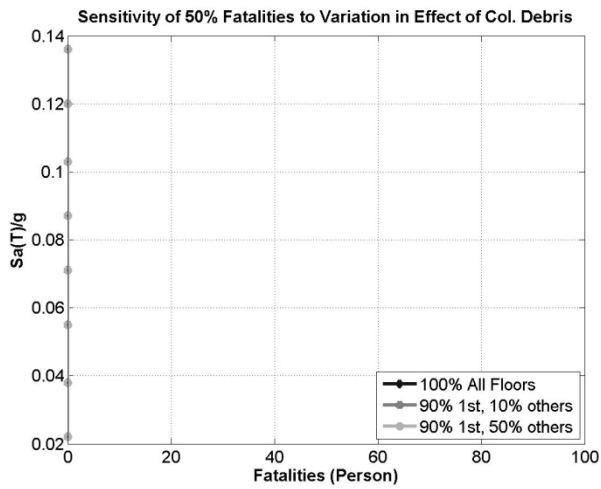


Figure 1-61 Number of fatalities curve estimated for variation in building collapse mode

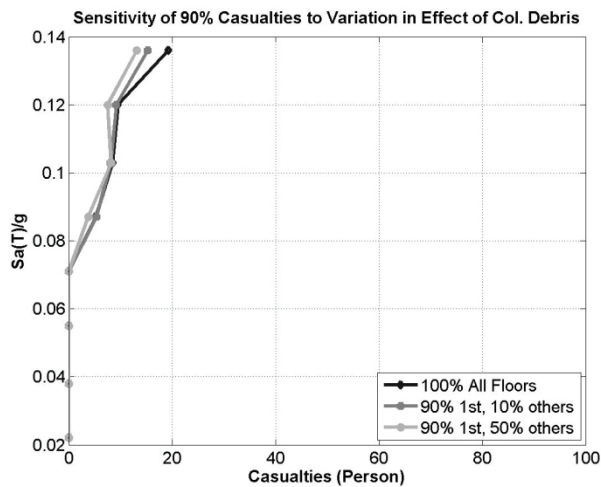


Figure 1-62 90% number of injuries estimated for variation in building collapse mode

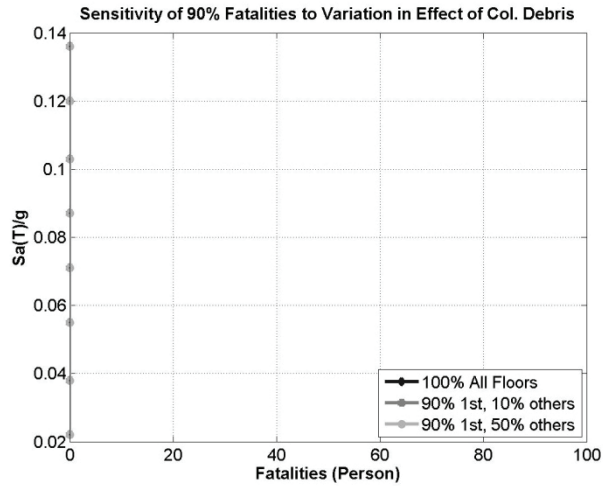


Figure 1-63 90% number of fatalities estimated for variation in building collapse mode

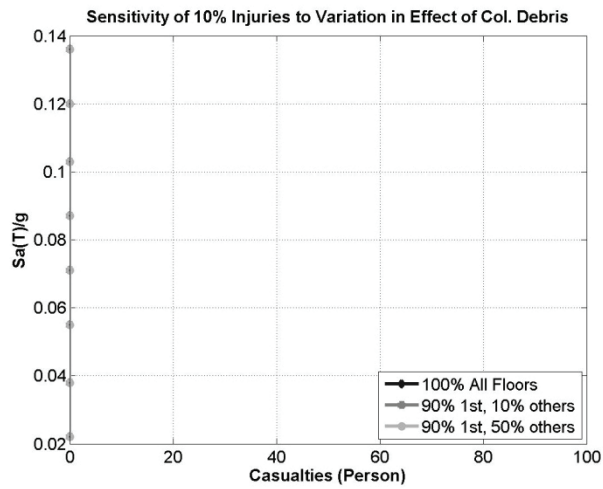


Figure 1-64 10% number of injuries estimated for variation in building collapse mode

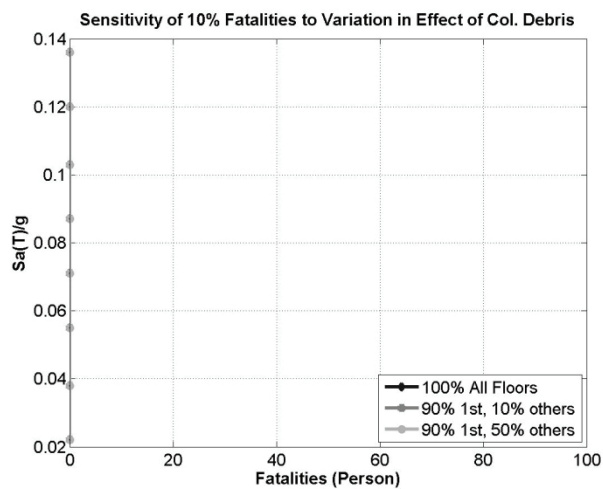


Figure 1-65 10% number of fatalities estimated for variation in building collapse mode

Table 1-9 Variation in Estimated Annualized Loss to Variation Building Collapse Mode

Case	Annualized Repair Cost	Annualized Repair Time	MAF. of Collapse	MAF of Red Tag
All 1 (Base Case)	\$26,573	0.58 Days	7.427 E-6	5.333 E-4
1 st story 0.9, others 0.1	\$22,270	0.50 Days	9.808 E-6	2.350 E-4
1 st story 0.9, others 0.5	\$22,240	0.49 Days	7.996 E-6	2.370 E-4

1.1.4.9 Sensitivity of loss predictions to variation in number of stripes used in time based analysis

We investigated using a smaller number of stripes for time base analysis. Figure 1-66 to Figure 1-71 show the difference between the 10%, 50%, and 90% fractiles of Repair Cost and Repair Time at various hazard levels. As can be seen, there is not much difference between the results; 4-stripes correspond to stripes number 1, 3, 5, 7 of the 8 stripes used in the base case; and stripes number 3 and 6 for the 2-stripes alternative. The only difference among loss curves are: 1) using larger number of stripes generates a loss curve with larger number of data points, 2) the difference between losses estimated at hazards shared among the base case, 4-stripes, and 2-stripes are merely from the inherent randomness in loss estimation process.

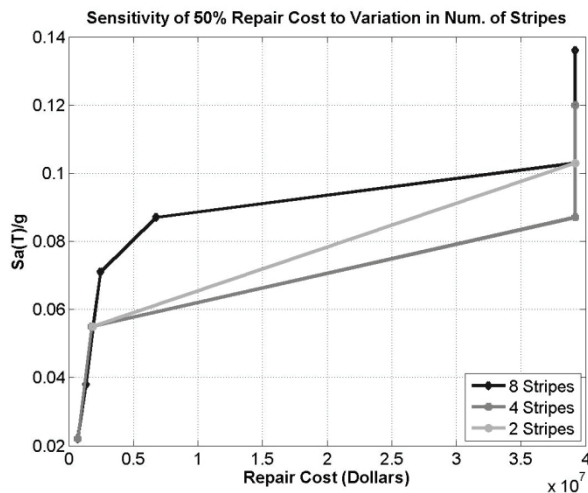


Figure 1-66 Median Repair Cost curve estimated for variation in number of stripes

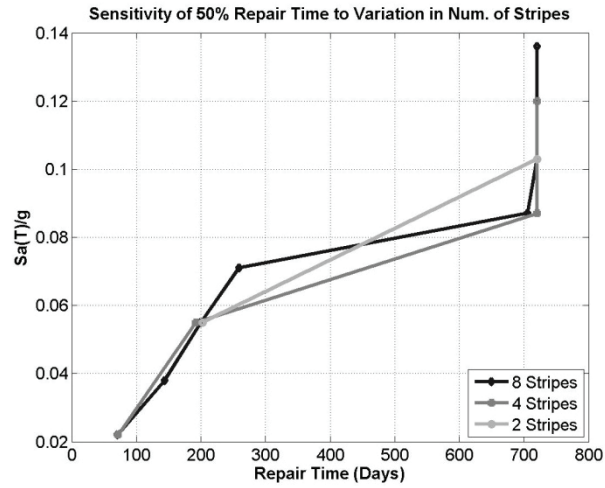


Figure 1-67 Median Repair Time curve estimated for variation in number of stripes

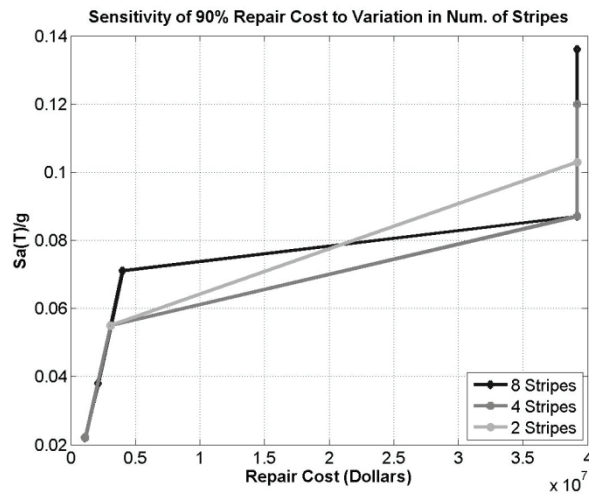


Figure 1-68 90% Repair Cost curve estimated for variation in number of stripes used

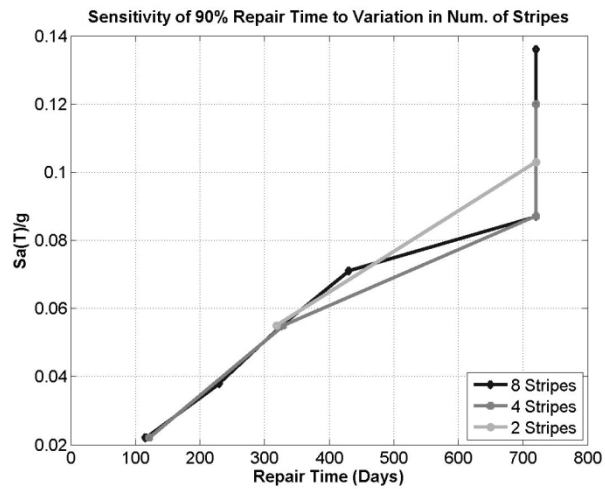


Figure 1-69 90% Repair Time curve estimated for variation in number of stripes

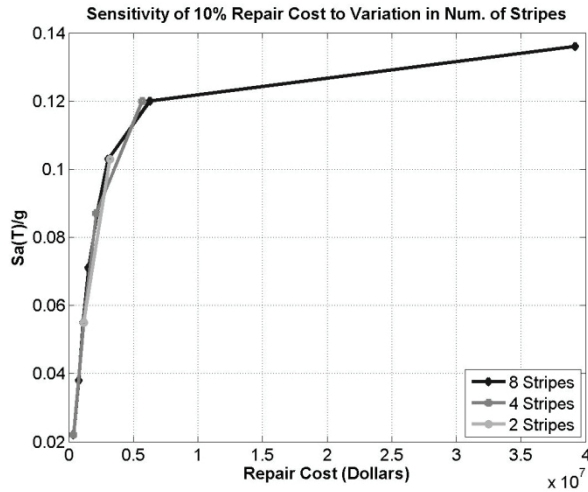


Figure 1-70 10% Repair Cost curve estimated for variation in number of stripes

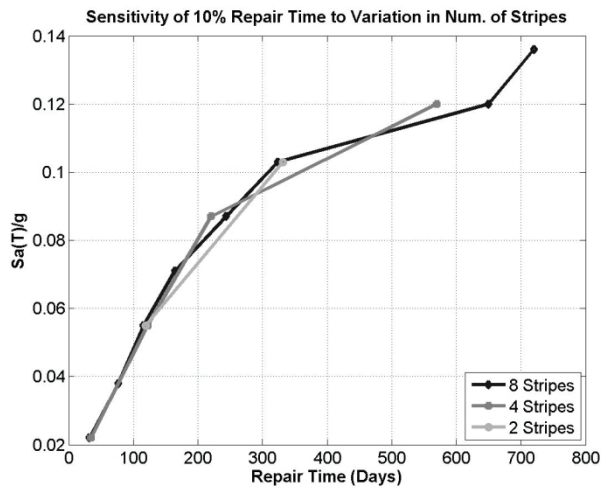


Figure 1-71 10% Repair Time curve estimated for variation in number of stripes

Table 1-10 shows the variation in annualized losses for various numbers of stripes used in the loss estimation process. The numbers indicate that using number of stripes smaller than 8 can lead to inaccurate estimates of annualized loss.

Table 1-10. Variation in Estimated Annualized Loss to Variation in Number of Stripes

Case	Annualized Repair Cost	Annualized Repair Time	MAF. of Collapse	MAF of Red Tag
8 Stripes (Base Case)	\$26,573	0.58 Days	7.427 E-6	5.333 E-4
4 Stripes	\$34,080	0.72 Days	8.579 E-6	4.935 E-4
2 Stripes	\$24,837	0.48 Days	18.20 E-6	3.472 E-4

1.1.4.10 Sensitivity of loss predictions to variation in analysis method.

The difference between the median estimates of losses, repair cost and repair time, using Simplified and Detailed analysis methods is negligible at high probability hazard levels where the structure essentially behaves elastic or moderately inelastic. Figures 1-72 and 1-73 show the variation of median repair cost and repair time, respectively, for Building A. In contrary, at lower probability hazard levels, median estimate of loss from two analysis methods are very different.

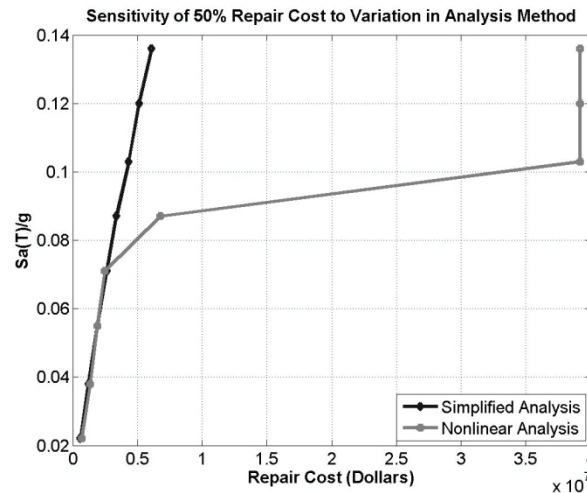


Figure 1-72 Median Repair Cost curve estimated for variation in analysis method

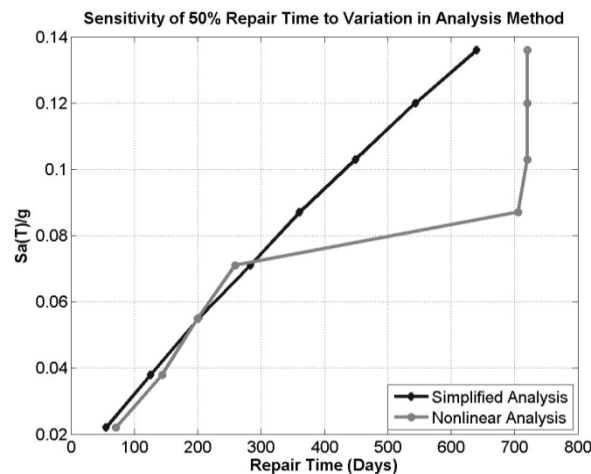


Figure 1-73 Median Repair Time curve estimated for variation in analysis method

10% and 90% fractiles of estimated repair cost and repair time show similar trends as of the median estimates. Figure 1-74 & Figure 1-75 show the 90%

loss values, and Figure 1-76 and Figure 1-77 show the 10% loss values. Investigation of these plots show that the variability in estimates of loss using the Detailed Analysis is larger than the variability in such estimates from the Simplified analysis. The loss value for 10% fractile at each hazard is smaller for the Detailed method; at 90% fractile, estimates losses is larger for the Detailed method.

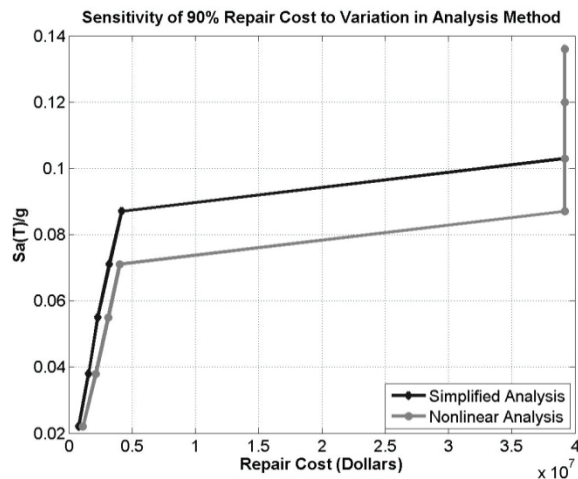


Figure 1-18 90% Repair Cost curve estimated for variation in analysis method

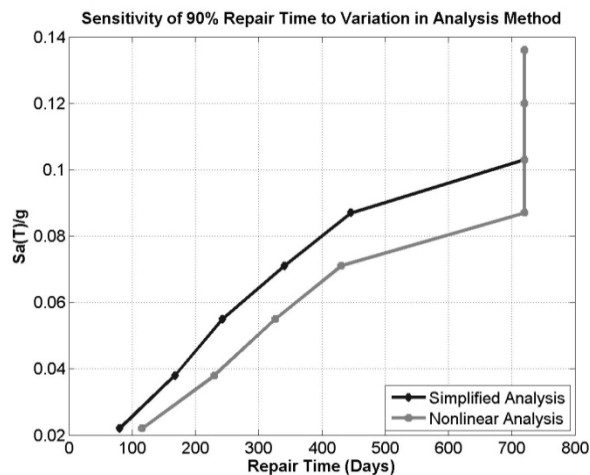


Figure 1-20 90% Repair Time curve estimated for variation in analysis method

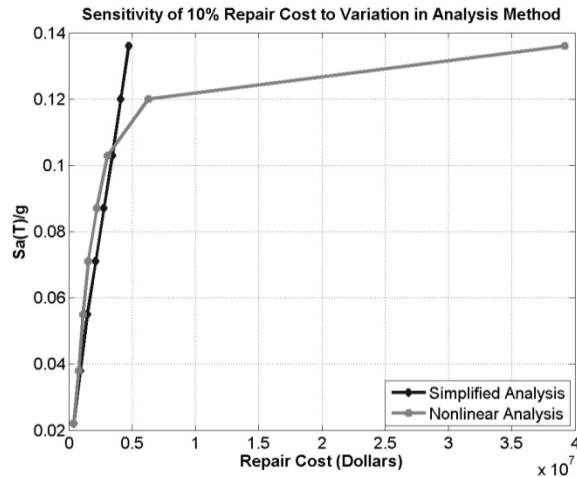


Figure 1-22 10% Repair Cost curve estimated for variation in analysis method

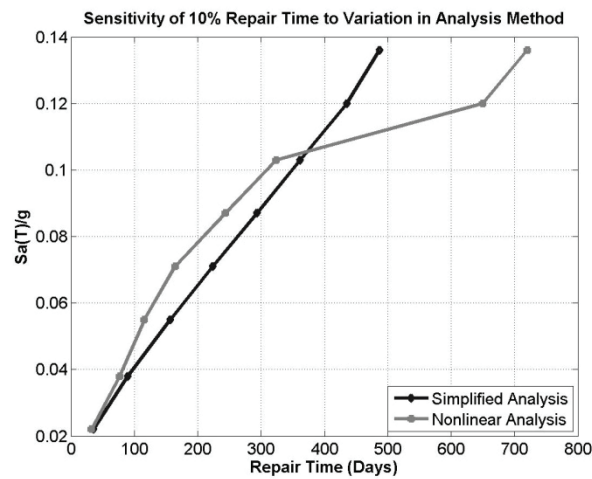


Figure 1-24 10% Repair Time curve estimated for variation in analysis method

Table 1-11 Variation in Estimated Annualized Loss to Variation in Analysis Method

Case	Annualized Repair Cost	Annualized Repair Time	MAF. of Collapse	MAF of Red Tag
Detailed (Base Case)	\$26,573	0.58 Days	7.427 E-6	5.333 E-4
Simplified	\$14,175	0.37 Days	5.151 E-6	0.477 E-4

1.1.7 Suggestions for Possible Improvements to the PACT Software

PACT is has made radical improvement from the last version. The following list should be counted as suggestion for improvement of the current program:

- The amount of data processed by PACT is large enough to cause memory problem for ordinary computers. Probably using advanced numerical techniques for the Monte Carlo simulation can extremely increase its application.
- Adding the flexibility of executing PACT in batch mode for extracting (exporting) data available in the “Examine Results” process can be much helpful.
- The hazard curve does not show a correct plot once 4 hazard levels instead of 8 are used in time-based analysis.

1.1.8 Appendix: Additional Studies

Additional studies were performed to further investigate PACT functionality and interrogate beta test results observed for all example buildings, as reported below.

Study #1. For checking the results of correlated versus non-correlated, provide results for 10th- and 90th-percentile results in addition to the mean values already provided for each intensity.

- Correlated performance groups were the only option that was used for Building A. The model is too large to run the non-correlated option.

Study #2. Investigate the following striping options and report result variations as MAFE for repair cost, repair time, casualties and red-tagging.

- 4-stripe approach averaging stripes 1 & 2, 3 & 4, 5 & 6 and 7 & 8.
- 3-stripe approach using stripes “0-2 (using 1 as the intensity)”, “3-5 (using 4 as the intensity)”, “6-8 (using 7 as the intensity)”. Note that we are extending the seismic hazard curve to an even lower intensity by adding the “0” intensity.

Summary of Results

No. of stripes	Variable	Value	Change
8 stripes (base case)	Probability of collapse	7.075 E-6	-
	Probability of red tagging	2.586 E-4	-
	Annualized cost (\$)	\$22,330	-
	Downtime (days)	0.50 Days	-
	Annualized fatalities	0.001	-
	Annualized injuries	0.0008	-
4 stripes *	Probability of collapse	8.579 E-6	21%
	Probability of red tagging	4.935 E-4	91%
	Annualized cost (\$)	\$34,080	53%
	Downtime (days)	0.72 Days	44%
	Annualized fatalities	0.0009	10%
	Annualized injuries	0.0016	100%
3 stripes [#]	Probability of collapse	10.271 E-6	45%
	Probability of red tagging	2.234 E-4	14%
	Annualized cost (\$)	\$30,944	39%
	Downtime (days)	0.68 Days	36%
	Annualized fatalities	0.0026	160%
	Annualized injuries	0.0014	75%
2 stripes [∞]	Probability of collapse	18.20 E-6	157%
	Probability of red tagging	3.472 E-4	34%
	Annualized cost (\$)	\$24,837	11%
	Downtime (days)	0.48 Days	4%
	Annualized fatalities	0.0042	320%
	Annualized injuries	0.0026	225%

* The results presented here correspond to the following case: stripes 1-2 (using 1 as the intensity), stripes 3-4 (using 3 as the intensity), stripes 5-6 (using 5 as the intensity), stripes 7-8 (using 7 as the intensity).

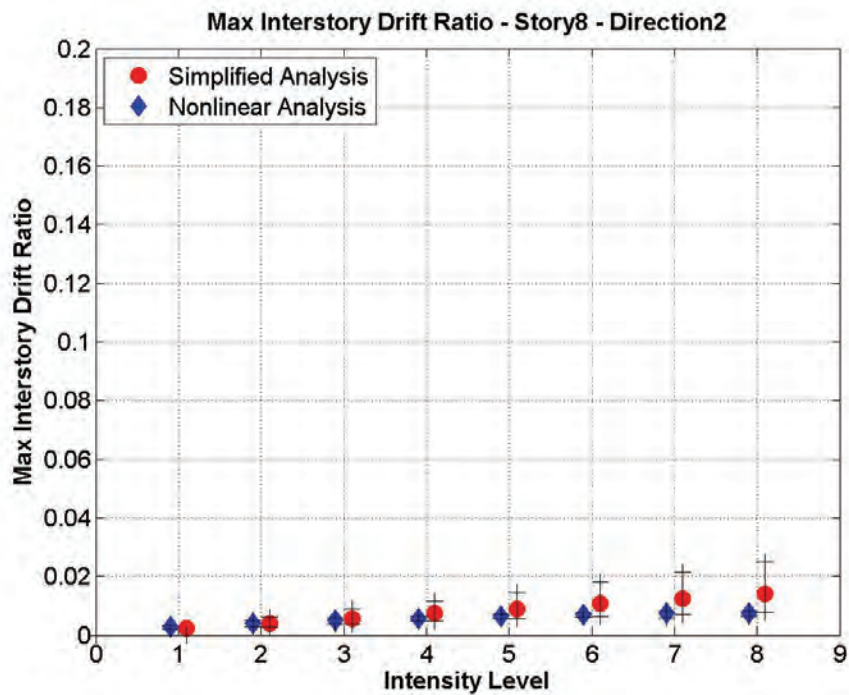
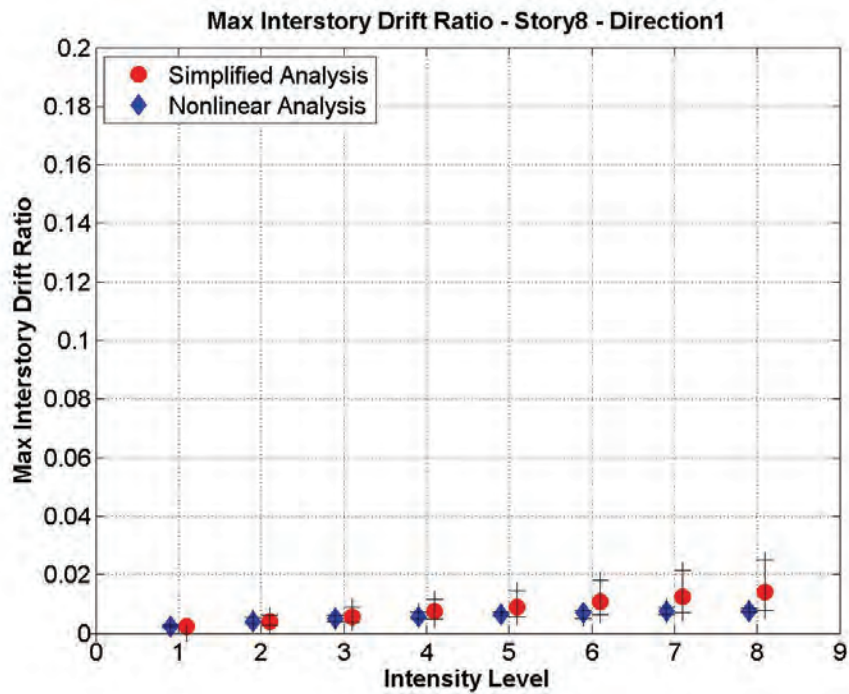
The results presented here correspond to the following case: stripes 1, 4, and 7.

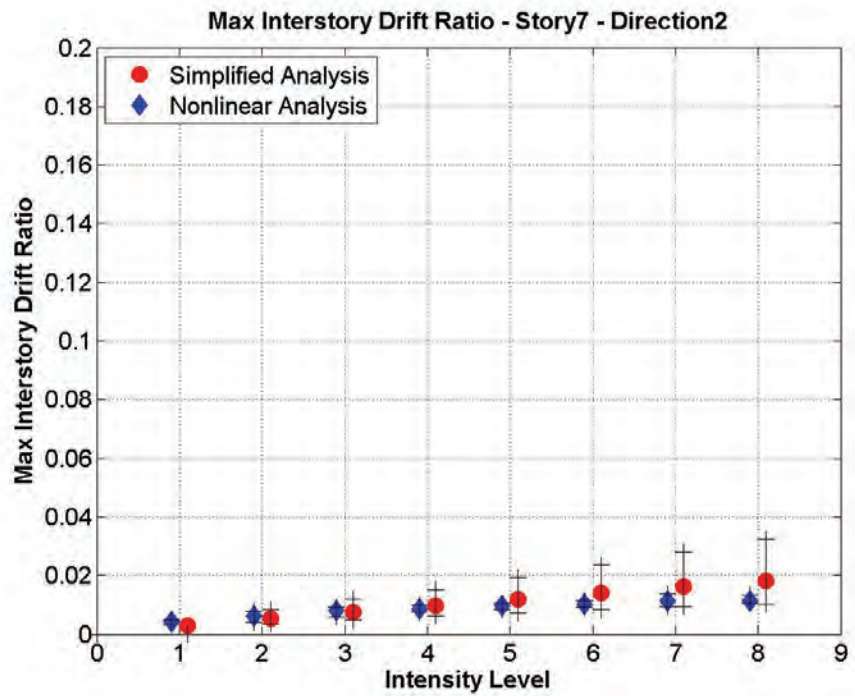
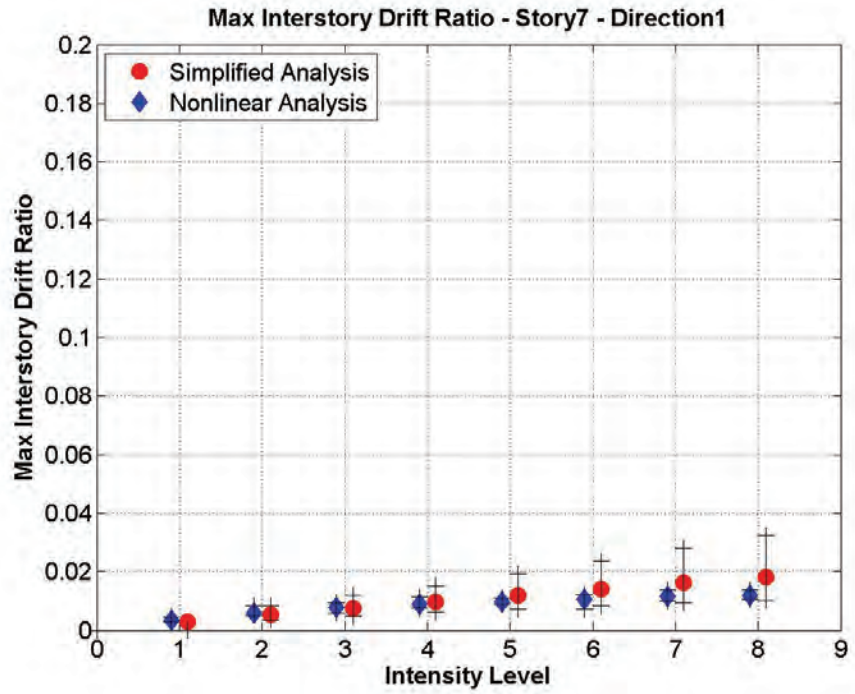
∞ The results presented here correspond to the following case: stripes 3, and 6

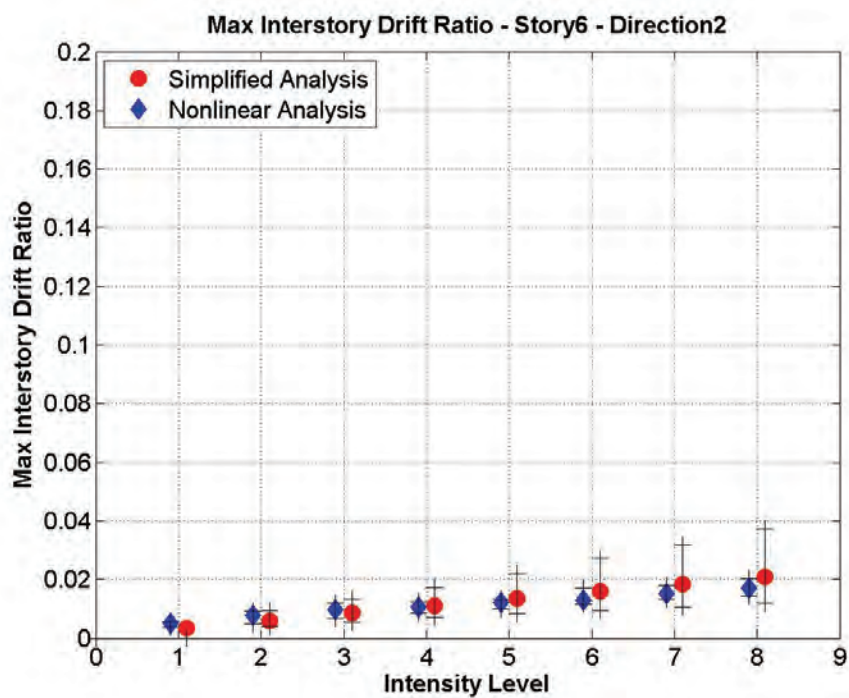
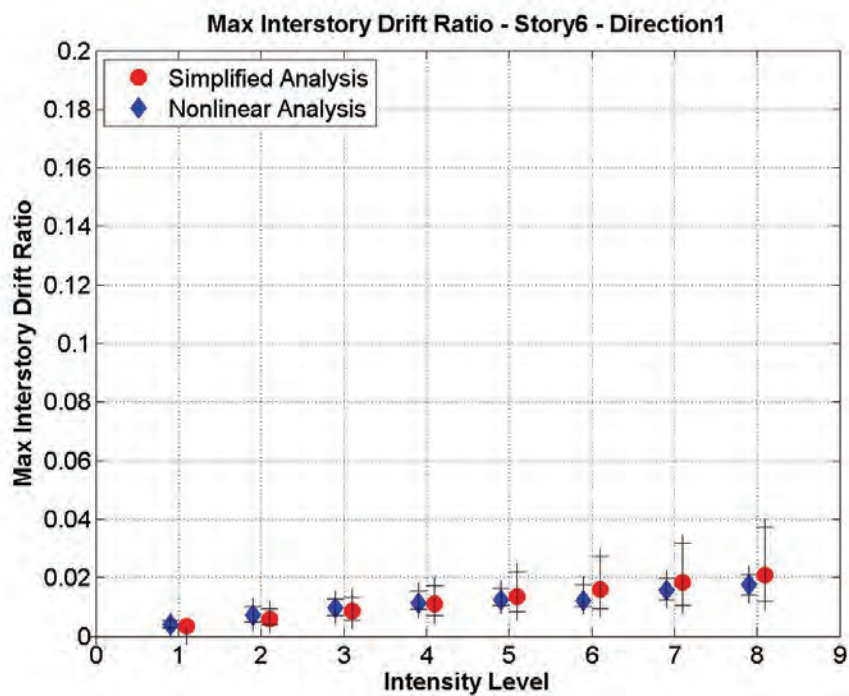
Study #3. Verify that the simple approach was used per the guidelines (provide specific factors) and provide the following comparisons between Simple and Nonlinear results:

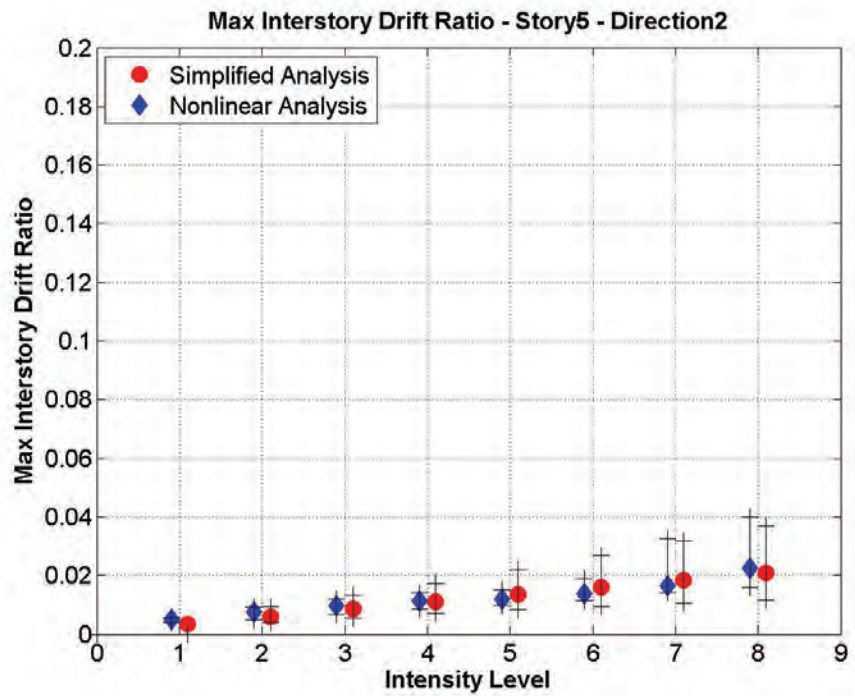
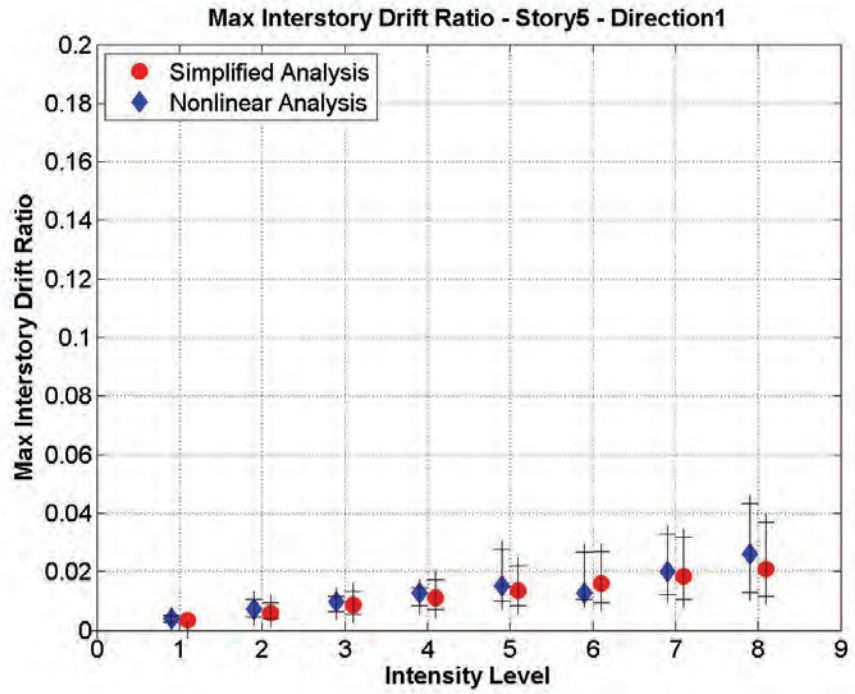
- Compare resulting demand parameters (story drift ratio and floor acceleration) for both the Simple and Nonlinear analyses side-by-side on a bar plot of floor vs. intensity (S_a).
- Provide individual plots for story drift ratio and floor acceleration, showing the results of the 10th, 50th and 90th percentiles (show as a range with the 50th percentile result as the “.” within the range).

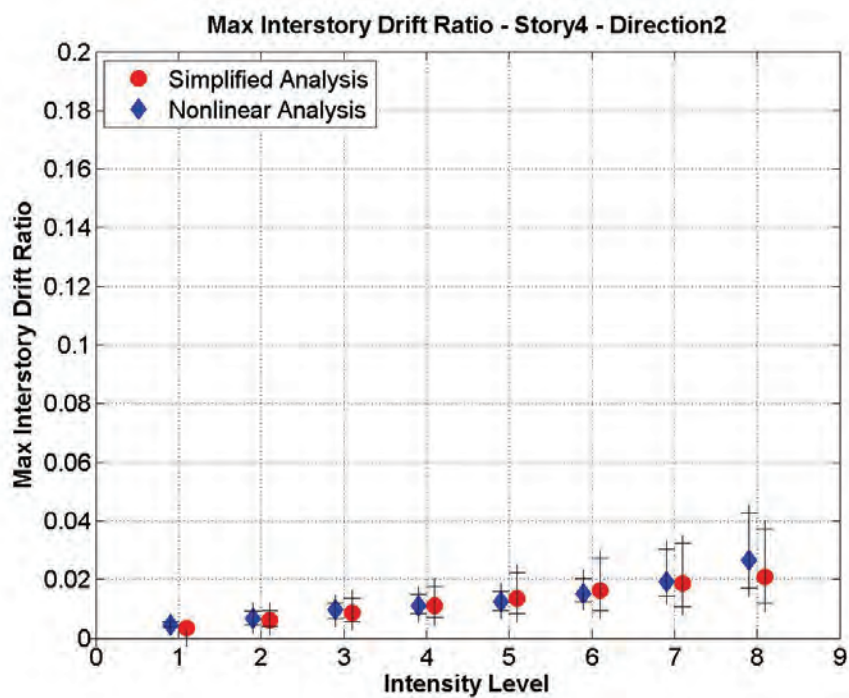
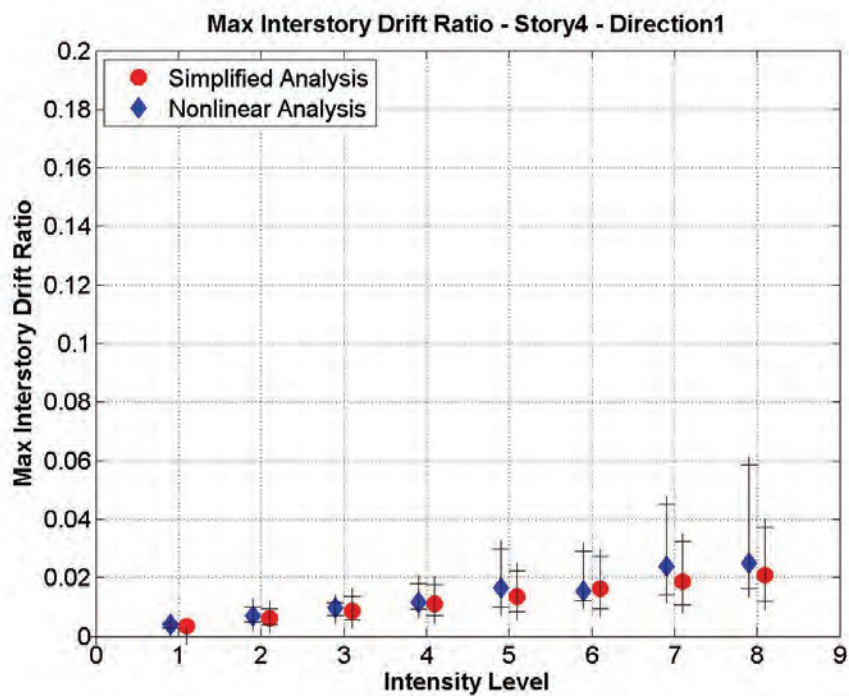
Plots of story drift ratio comparisons (Study #3):

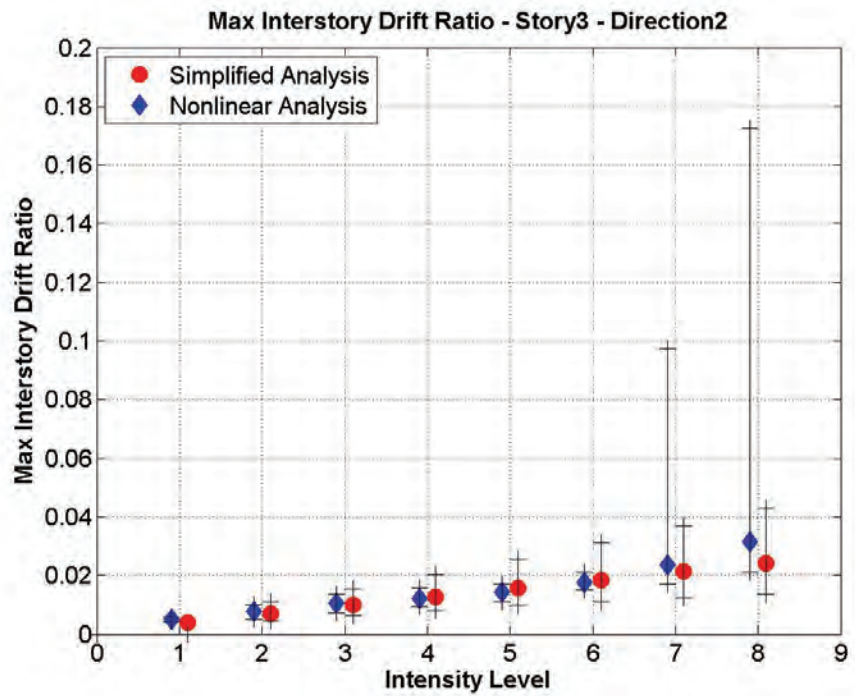
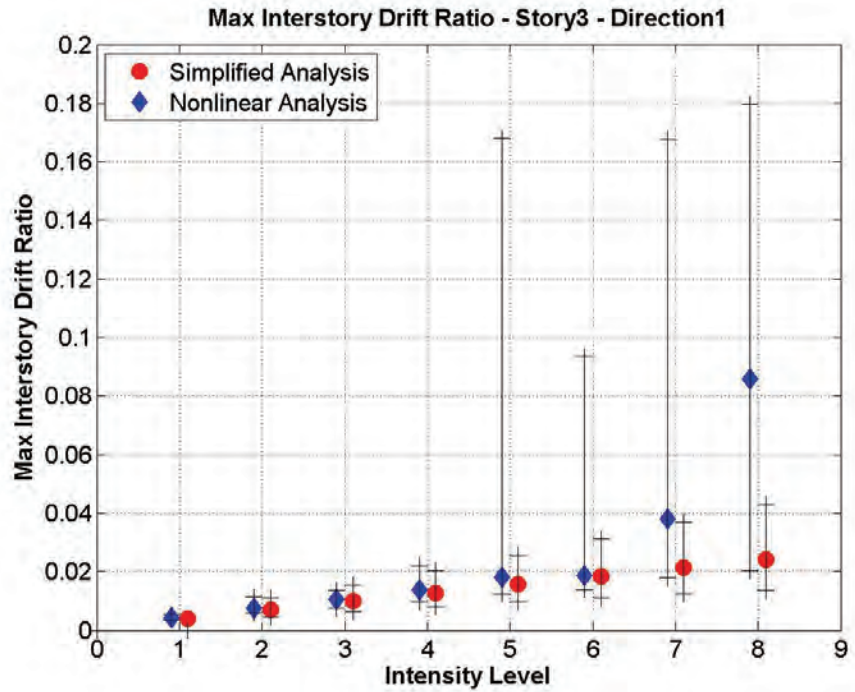


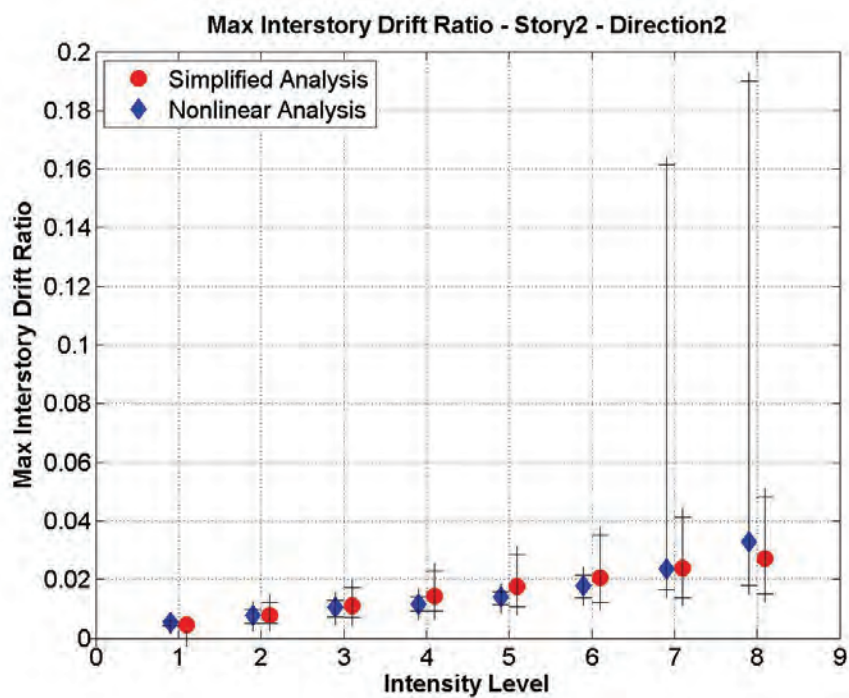
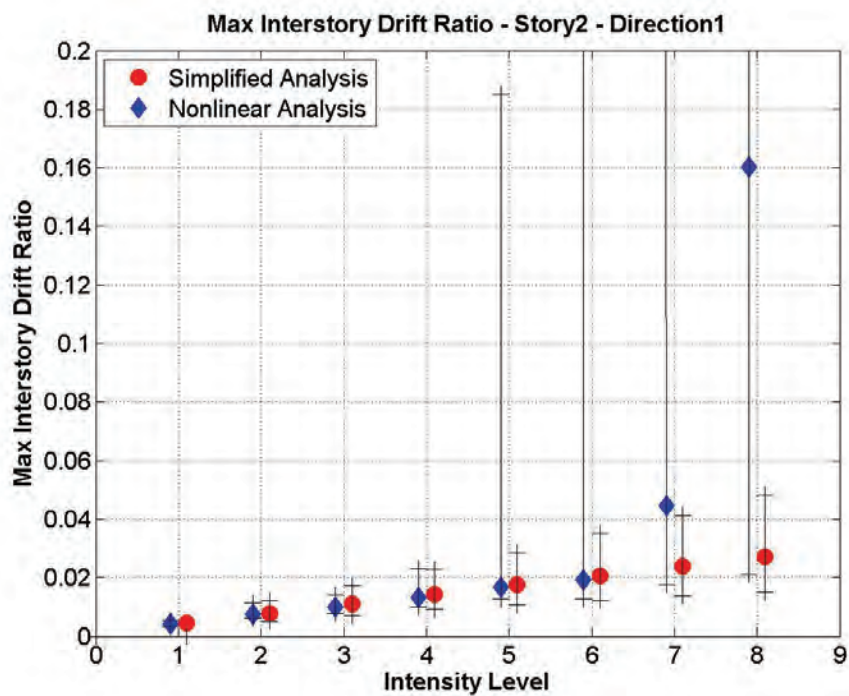


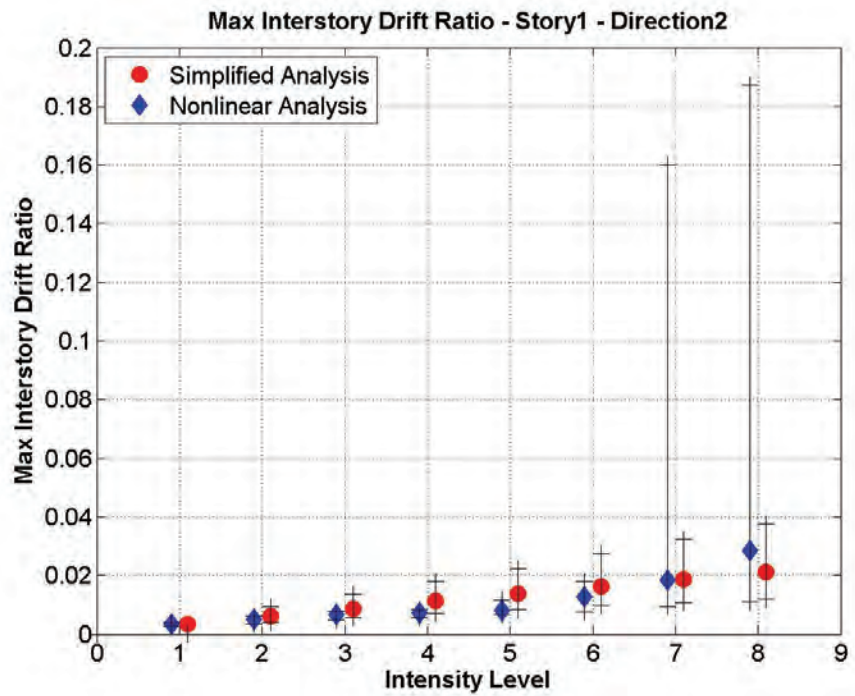
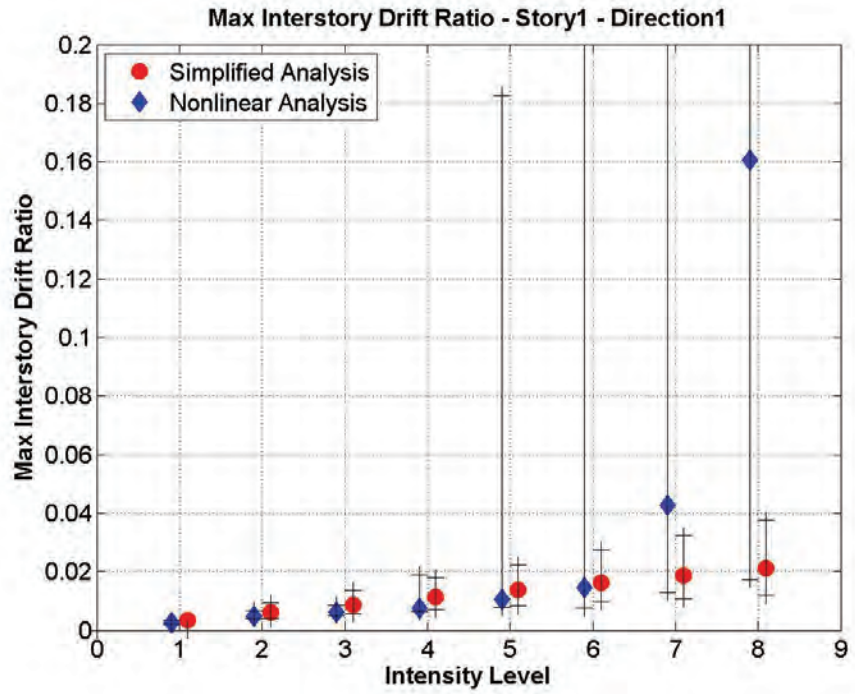




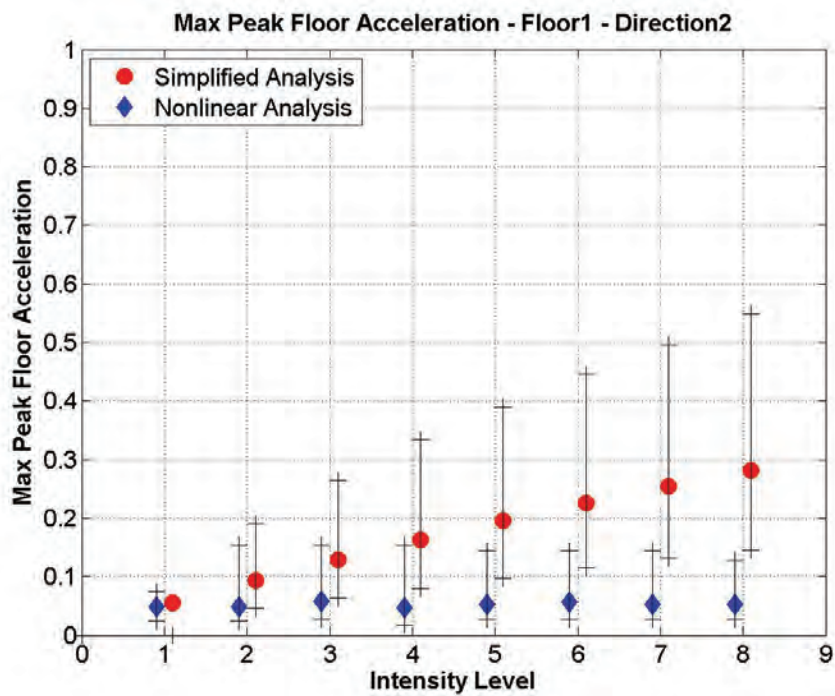
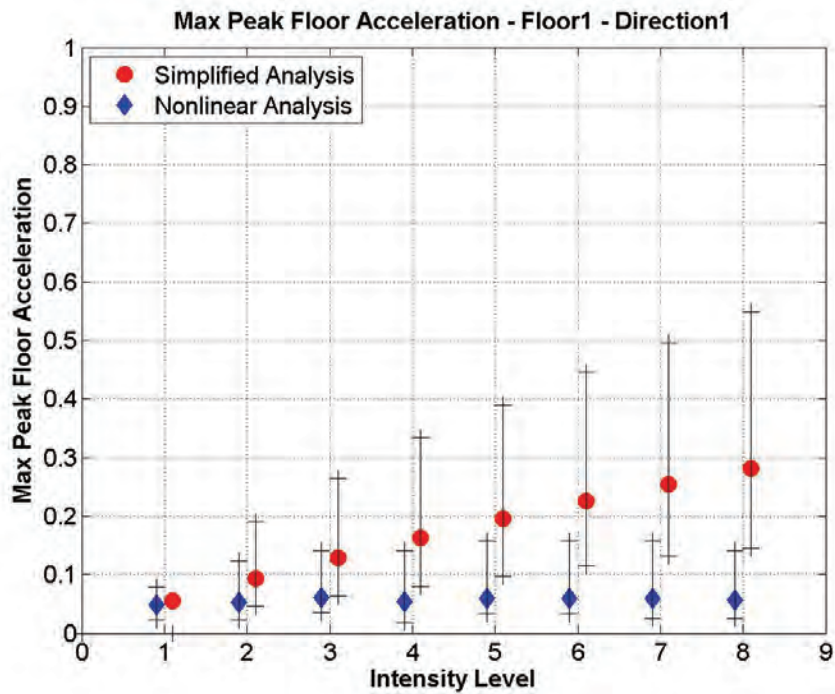


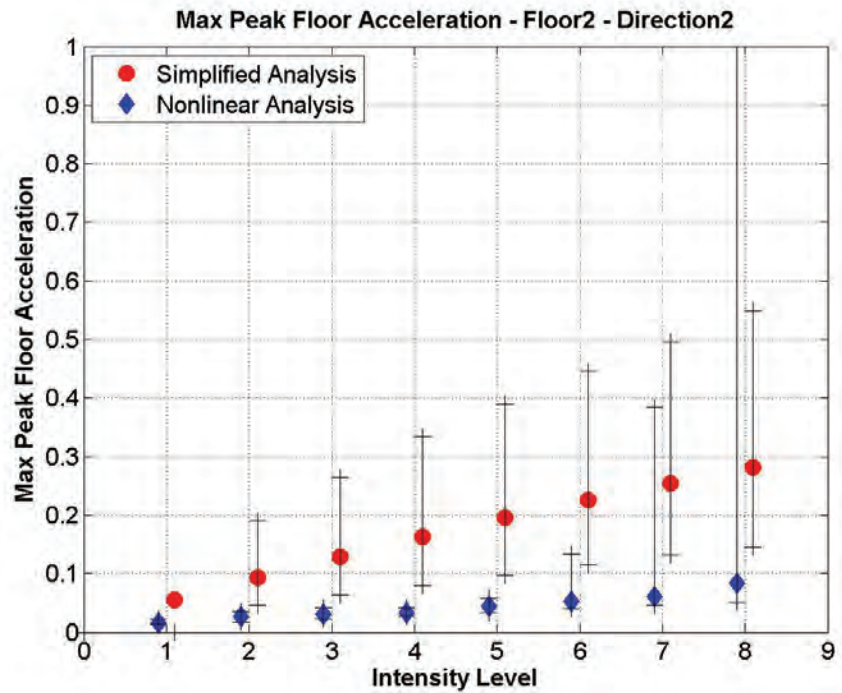
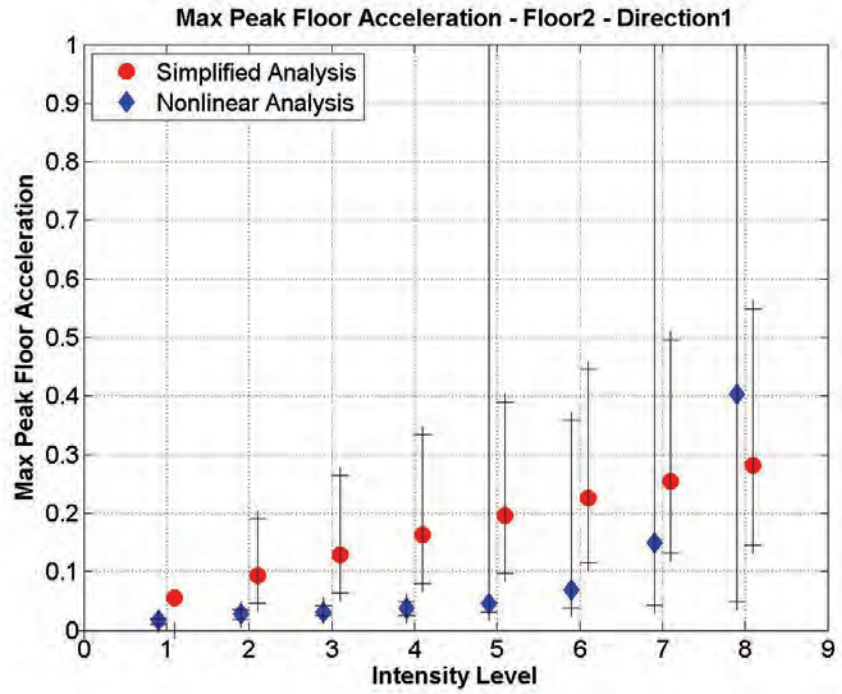


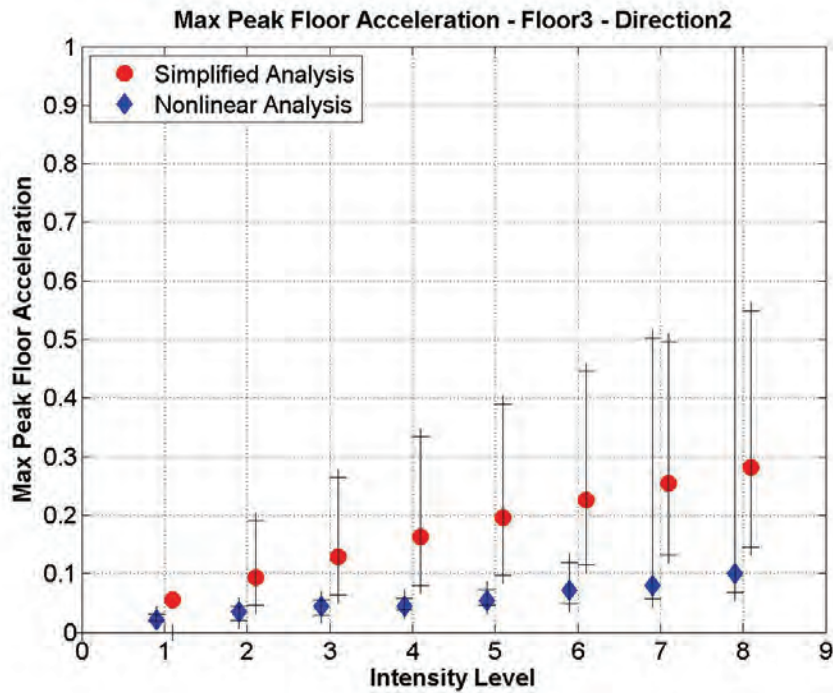
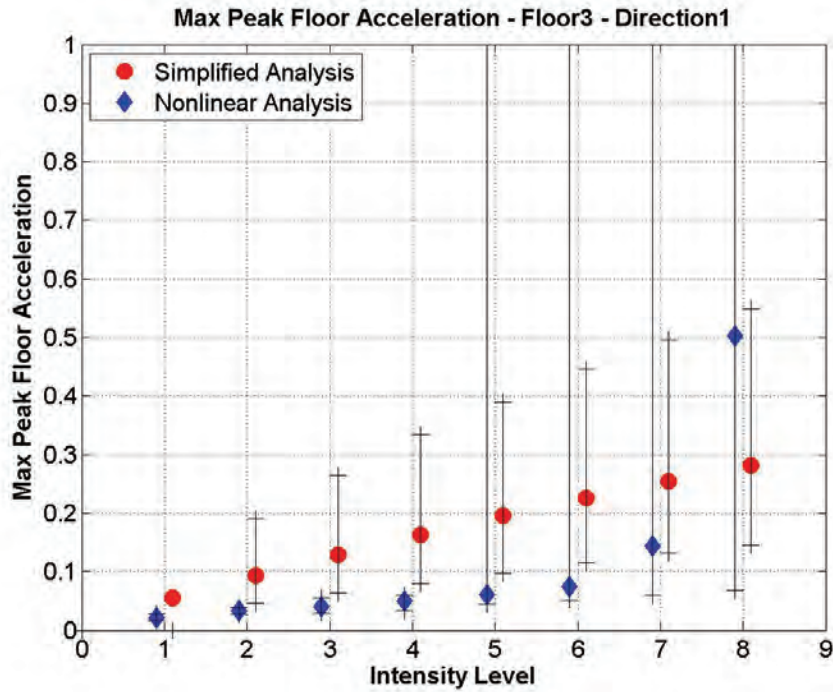


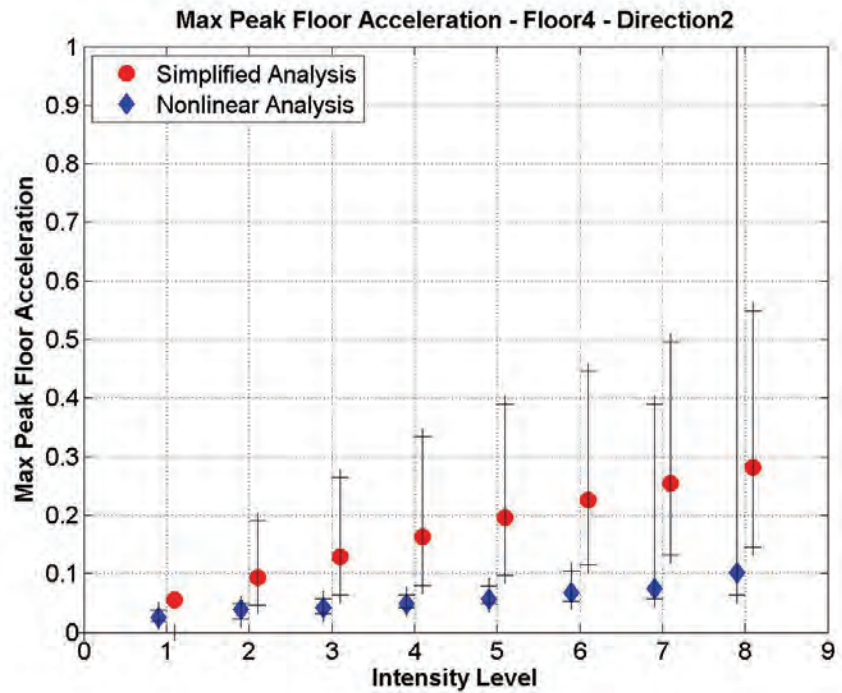
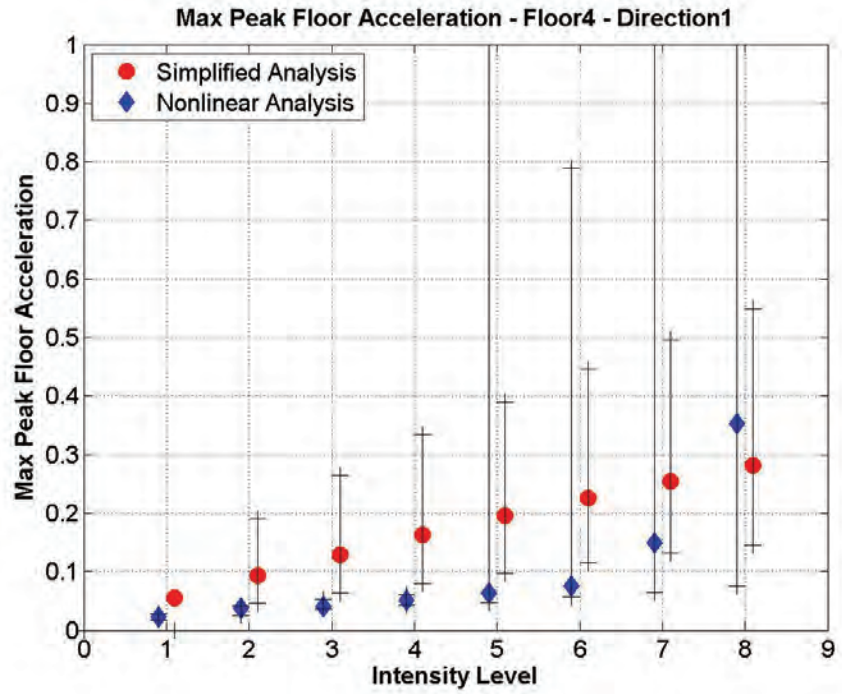


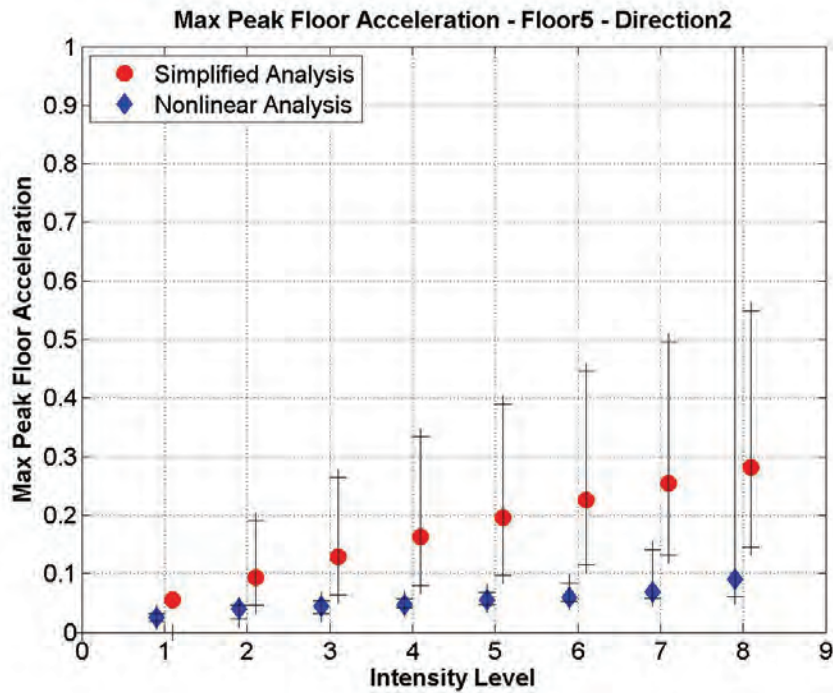
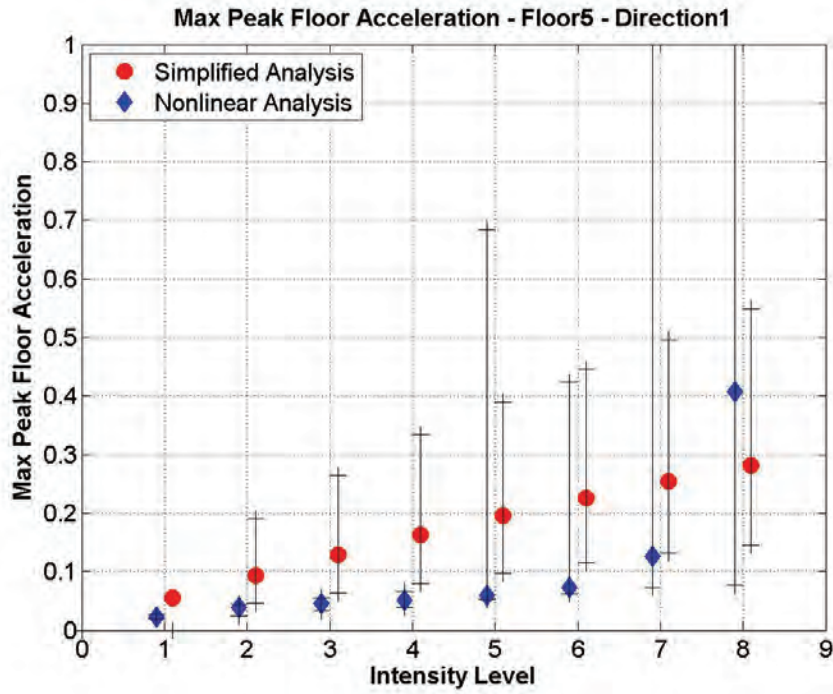
Plots of floor acceleration comparisons (Study #3):

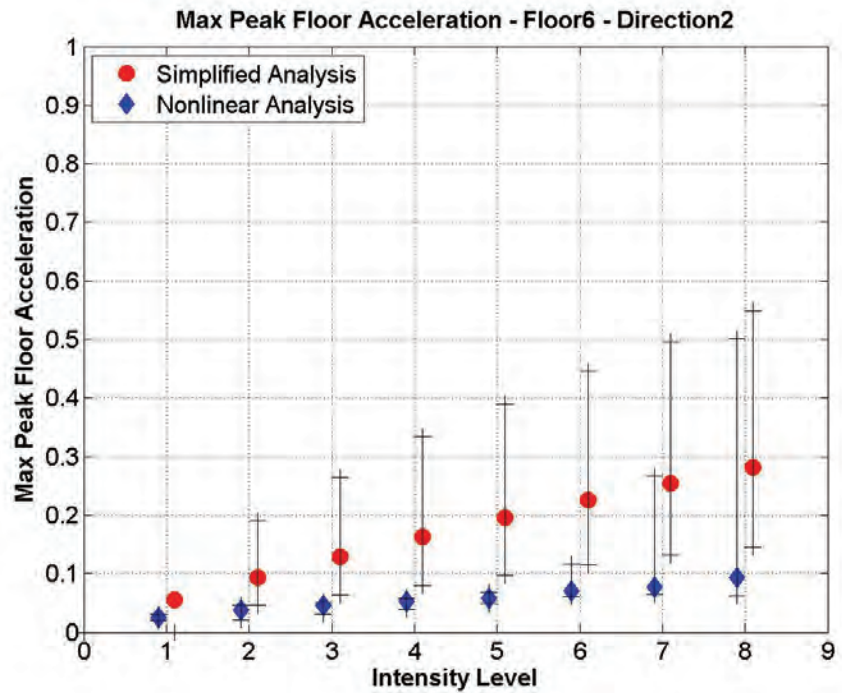
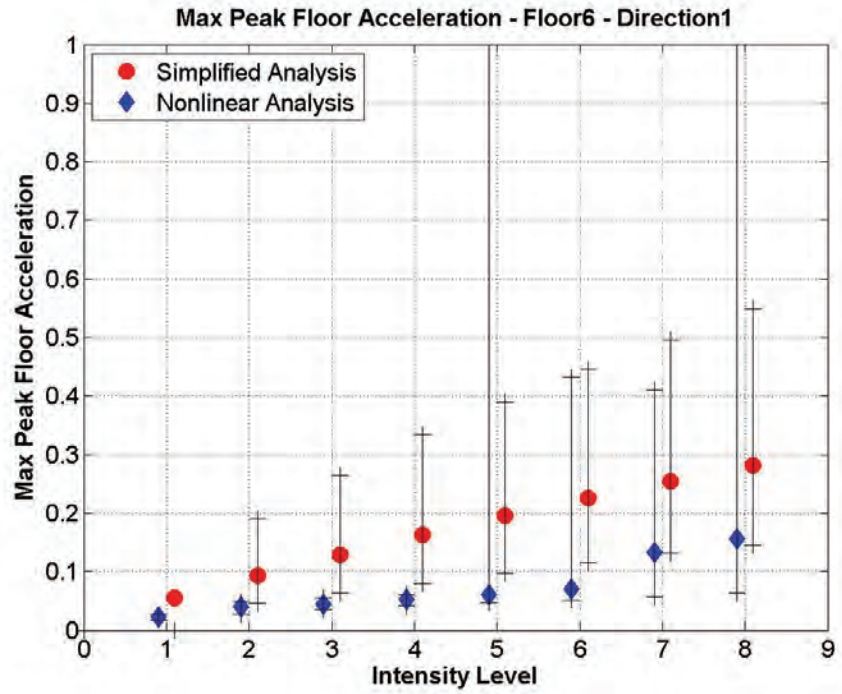


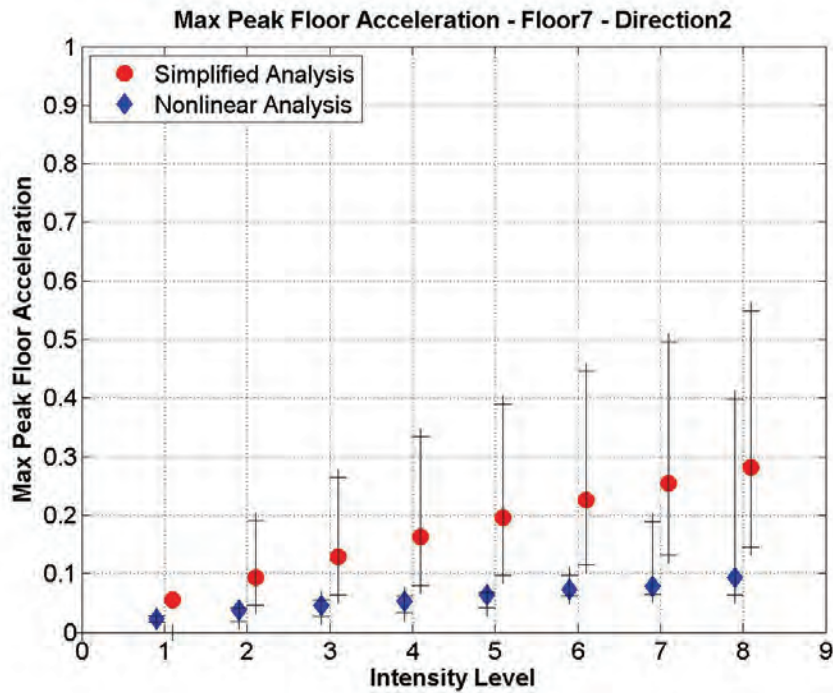
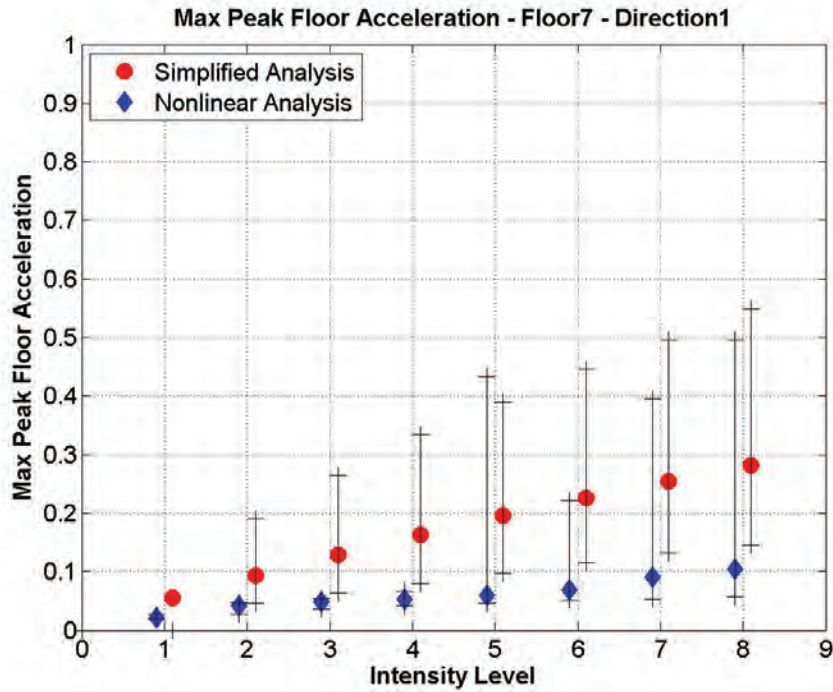


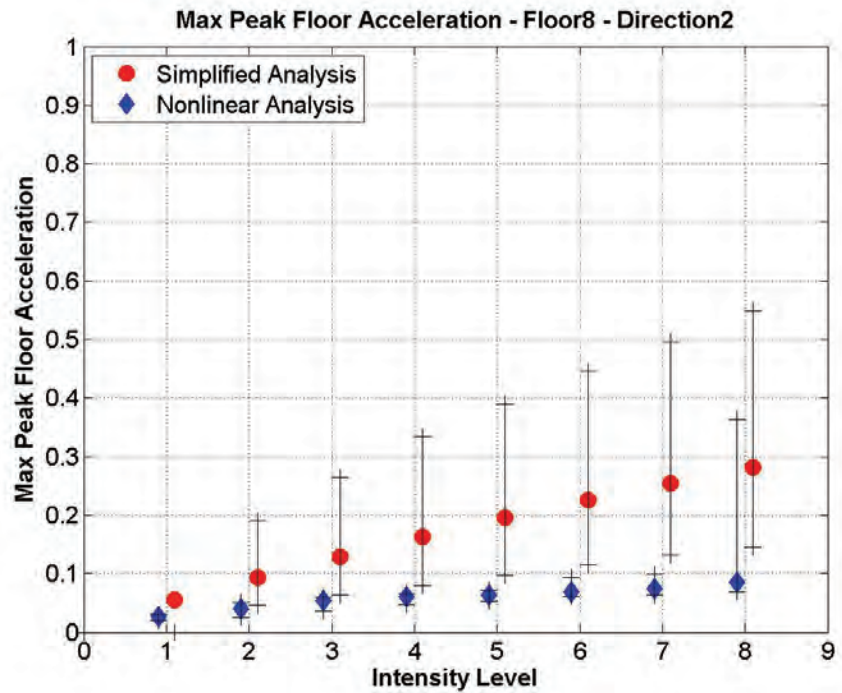
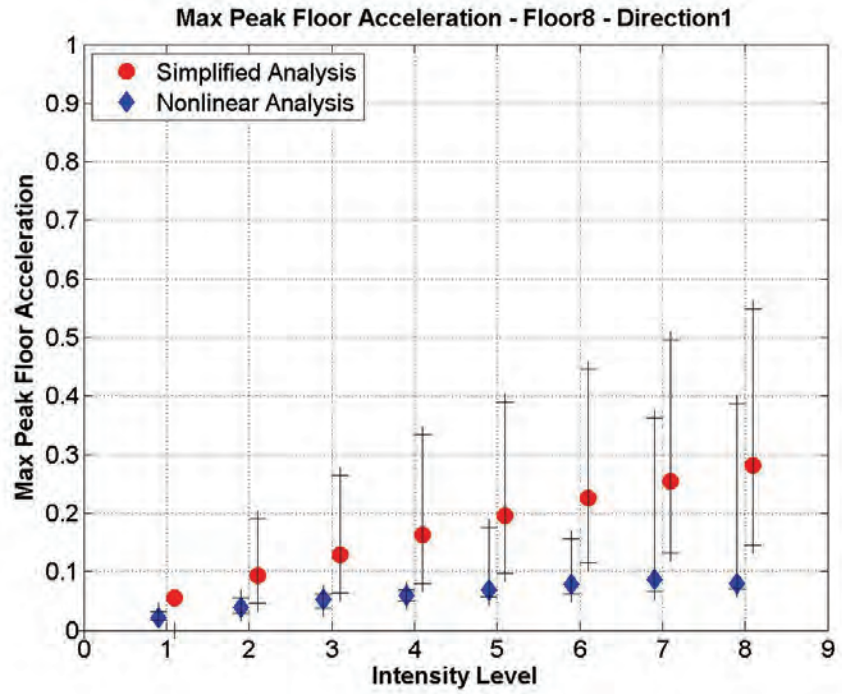


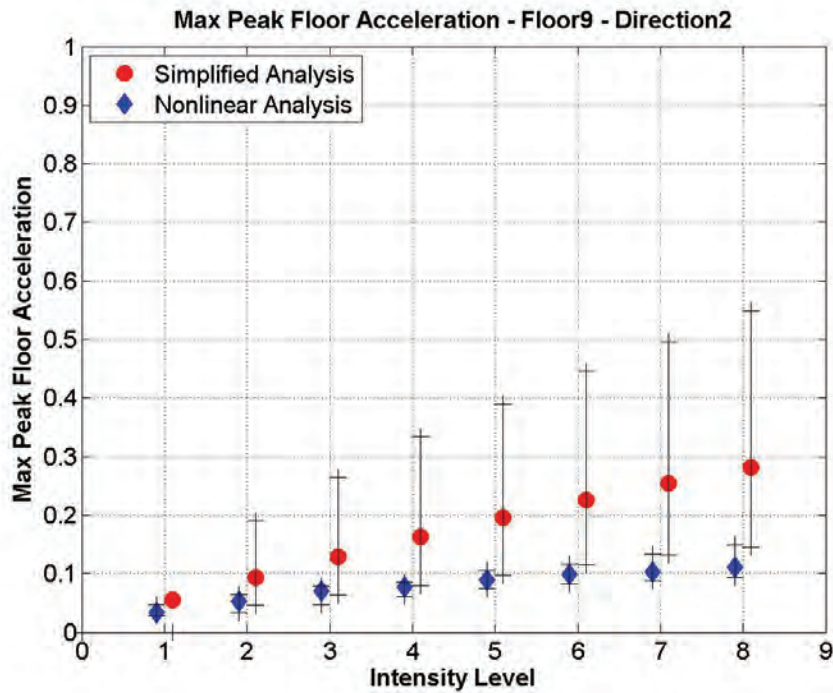
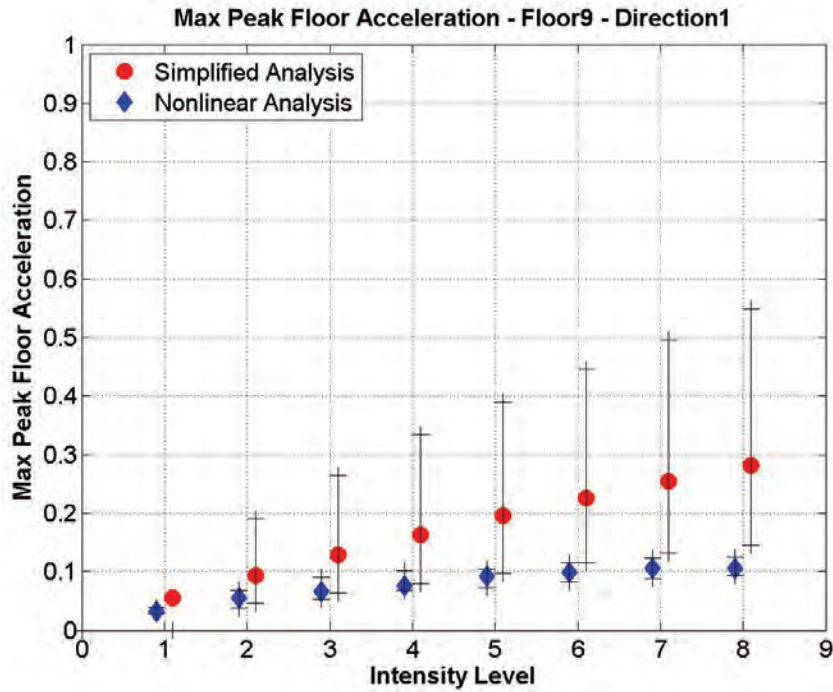




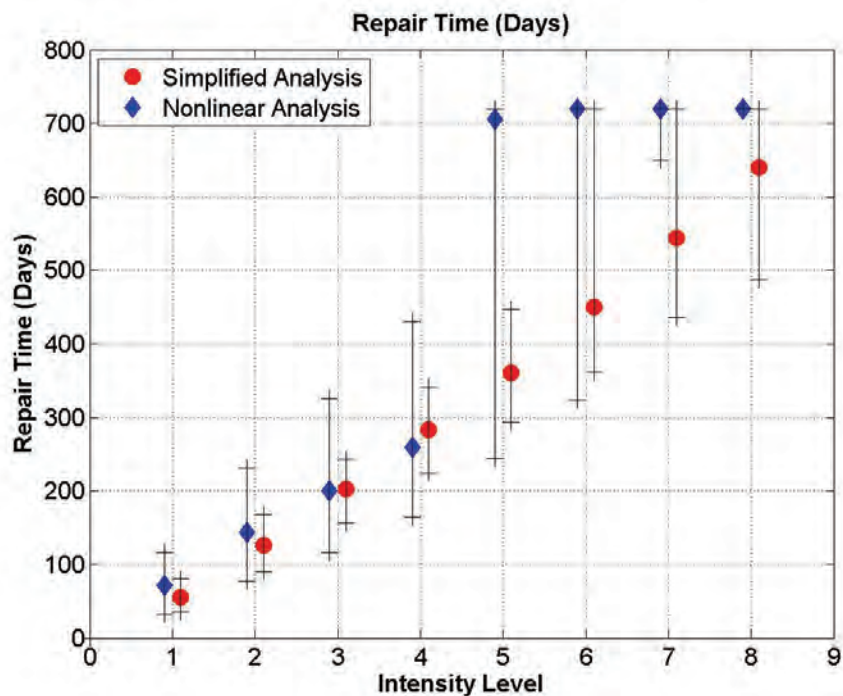
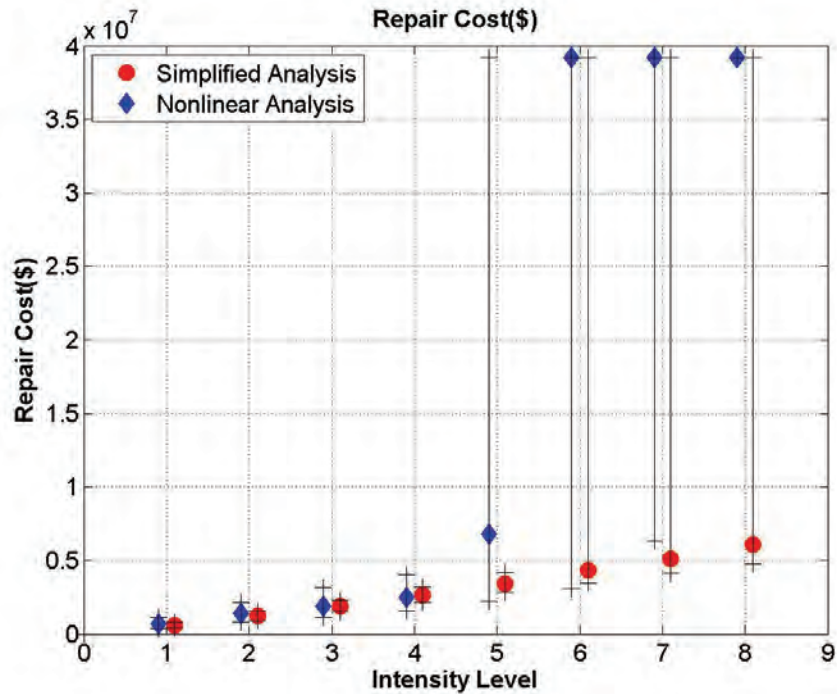


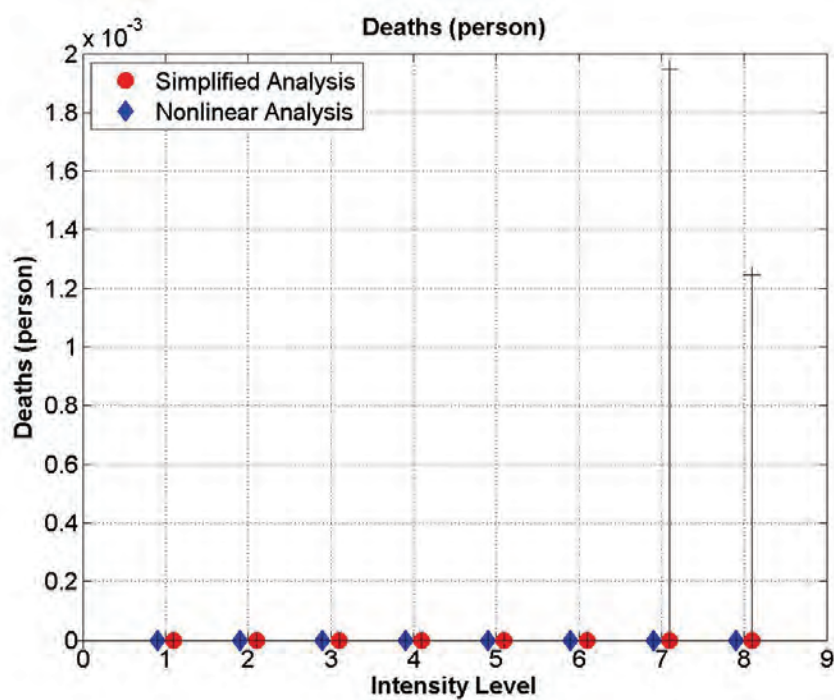
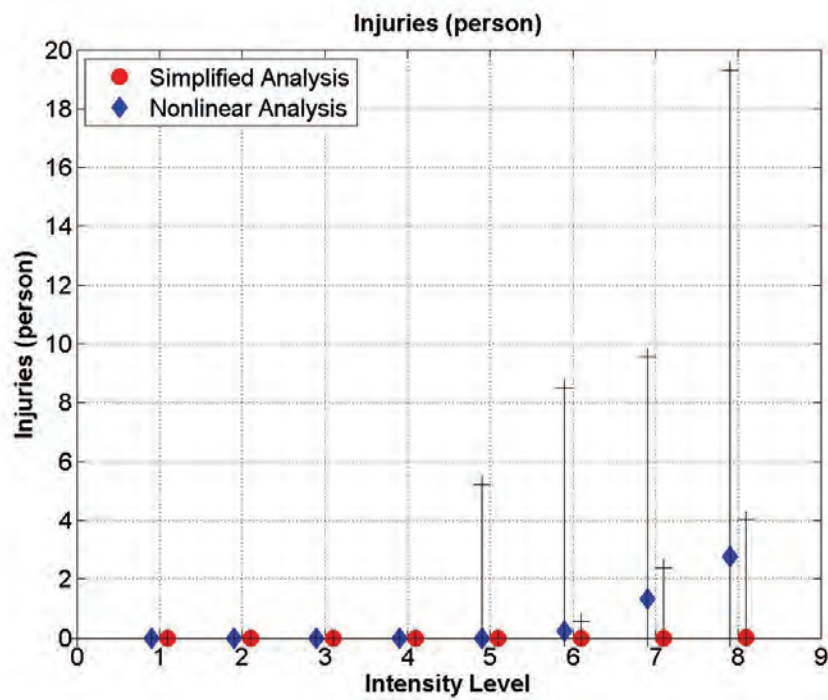






Study #4. Compare the resulting consequences (repair cost, repair time, and casualties) for both the Simple and Nonlinear analyses side-by-side on a bar plot of consequence result vs. intensity (Sa). Provide an individual plot for each consequence, showing the 10th, 50th and 90th percentiles (show as a range with the 50th percentile result as the “.” within the range).





Study #5. Report the effect of modeling dispersion on the 10th and 90th percentiles (in addition to the mean values shown) for each intensity.

Summary of Results

Int.	Variable	Model dispersion: 0.35 (base case)			Model dispersion: 0.14			Model dispersion: 0.5		
		Mean	10 th percentile	90 th percentile	Mean	10 th percentile	90 th percentile	Mean	10 th percentile	90 th percentile
1	Repair Cost (\$)	\$695,007.8	\$377,151.2	\$1,116,020.4	\$675,861.4	\$445,229.2	\$990,388.3	\$751,557.7	\$311,059.2	\$1,715,250.7
	Repair time (days)	71.3	32.5	116.0	65.3	40.0	103.8	72.9	27.4	179.1
	No. of Fatalities	0.00000	0.00000	0.00000	0.00000	0.00000	0.00000	0.00000	0.00000	0.00000
	No. of Injuries	0.00000	0.00000	0.00000	0.00000	0.00000	0.00000	0.00000	0.00000	0.00000
2	Repair Cost (\$)	\$1,373,969.0	\$781,410.9	\$2,143,825.6	\$1,358,329.5	\$901,311.9	\$2,028,690.6	\$1,725,802.5	\$714,476.1	\$3,627,066.5
	Repair time (days)	143.8	77.1	230.5	147.6	90.4	211.0	179.8	69.8	375.9
	No. of Fatalities	0.00000	0.00000	0.00000	0.00000	0.00000	0.00000	0.00000	0.00000	0.00000
	No. of Injuries	0.00000	0.00000	0.00000	0.00000	0.00000	0.00000	0.00000	0.00000	0.00000
3	Repair Cost (\$)	\$1,894,293.6	\$1,127,758.3	\$3,132,770.7	\$1,841,036.7	\$1,310,422.2	\$2,739,491.9	\$2,096,084.1	\$958,496.3	\$5,759,660.1
	Repair time (days)	200.2	116.1	326.1	196.7	137.6	294.7	222.0	100.0	578.5
	No. of Fatalities	0.00000	0.00000	0.00000	0.00000	0.00000	0.00000	0.00000	0.00000	0.00000
	No. of Injuries	0.00000	0.00000	0.00000	0.00000	0.00000	0.00000	0.00000	0.00000	0.00000
4	Repair Cost (\$)	\$2,488,563.1	\$1,542,400.4	\$4,026,375.1	\$2,457,341.5	\$1,562,700.3	\$3,306,969.4	\$2,949,145.5	\$1,414,366.2	\$6,524,506.9
	Repair time (days)	259.0	164.7	430.8	262.7	165.5	347.0	308.2	146.8	671.3
	No. of Fatalities	0.00000	0.00000	0.00000	0.00000	0.00000	0.00000	0.00000	0.00000	0.00000
	No. of Injuries	0.00000	0.00000	0.00000	0.00000	0.00000	0.00000	0.00000	0.00000	0.00000
5	Repair Cost (\$)	\$6,783,689.3	\$2,230,737.6	\$39,200,000.0	\$6,716,241.5	\$2,326,035.3	\$39,200,000.0	\$10,866,483.0	\$2,463,878.3	\$39,200,000.0
	Repair time (days)	705.6	243.7	720.0	696.9	253.6	720.0	720.0	256.2	720.0
	No. of Fatalities	0.00000	0.00000	0.00000	0.00000	0.00000	0.00000	0.00000	0.00000	0.00000
	No. of Injuries	0.00000	0.00000	5.23794	0.00000	0.00000	4.72421	0.00000	0.00000	7.12385
6	Repair Cost (\$)	\$39,200,000.0	\$3,075,936.4	\$39,200,000.0	\$39,200,000.0	\$3,328,629.2	\$39,200,000.0	\$39,200,000.0	\$3,108,772.2	\$39,200,000.0
	Repair time (days)	720.0	323.8	720.0	720.0	343.9	720.0	720.0	321.5	720.0
	No. of Fatalities	0.00000	0.00000	0.00000	0.00000	0.00000	0.00000	0.00000	0.00000	0.00125
	No. of Injuries	0.24147	0.00000	8.50353	0.00000	0.00000	5.61364	0.59978	0.00000	9.28969
7	Repair Cost (\$)	\$39,200,000.0	\$6,294,889.1	\$39,200,000.0	\$39,200,000.0	\$6,755,339.3	\$39,200,000.0	\$39,200,000.0	\$5,607,948.7	\$39,200,000.0
	Repair time (days)	720.0	649.9	720.0	720.0	653.1	720.0	720.0	584.6	720.0
	No. of Fatalities	0.00000	0.00000	0.00000	0.00000	0.00000	0.00000	0.00000	0.00000	34.04209
	No. of Injuries	1.33051	0.00000	9.55866	1.18793	0.00000	12.58021	1.99430	0.00000	15.56611
8	Repair Cost (\$)	\$39,200,000.0	\$39,200,000.0	\$39,200,000.0	\$39,200,000.0	\$39,200,000.0	\$39,200,000.0	\$39,200,000.0	\$39,200,000.0	\$39,200,000.0
	Repair time (days)	720.0	720.0	720.0	720.0	720.0	720.0	720.0	720.0	720.0
	No. of Fatalities	0.00000	0.00000	0.00000	0.00000	0.00000	0.00000	0.00000	0.00000	64.26561
	No. of Injuries	2.75671	0.00000	19.30069	2.28466	0.00000	15.89046	3.06884	0.00000	21.14847

Plots of dispersion comparisons for each consequence (Study #5):

